TITLE
Remote sensing restores predictability of ectotherm body temperature in the world's forests

RUNNING TITLE:
Remote sensing and body temperature

AUTHORS
Adam C. Algar (corresponding author)
School of Geography, University of Nottingham, Nottingham, NG7 2RD, United Kingdom
adam.algar@nottingham.ac.uk
+44 (0)115 9515459

Kate Morley
School of Geography, University of Nottingham, Nottingham, NG7 2RD, United Kingdom
kate.morley0@gmail.com

Doreen S. Boyd
School of Geography, University of Nottingham, Nottingham, NG7 2RD, United Kingdom
doreen.boyd@nottingham.ac.uk

ACKNOWLEDGEMENTS
We thank M. Stevens, R. Freckleton, R. Field, D. Pincheira-Donoso, S. Tarr, and J.J. Hicks for helpful guidance and feedback.

BIOSKETCH
Adam C. Algar's research asks how organisms respond ecologically and evolutionarily to climate across spatial scales.
Kate Morley's MSc integrated remote sensing data into macrophysiology.
Doreen S. Boyd's main research interests are in the optimal exploitation of remote sensing systems to understand ecosystem services provided by terrestrial systems.

ABSTRACT

AIM: Rising global temperatures are predicted to increase ectotherms' body temperatures, benefitting some species but threatening others. Biophysical models predict a key role for shade in buffering these effects, but the difficulty of measuring shade across broad spatial extents limits predictions of ectotherms' thermal futures at the global scale. Here, we extend biophysical models of ectotherm body temperature to include effects of forest canopy shade, via leaf area index, and test whether considering remotely-sensed canopy density improves predictions of body temperature variation in heavily shaded habitats.

LOCATION: Worldwide.

TIME PERIOD: 1990–2010.

MAJOR TAXA STUDIED: Lizards.

METHODS: We test predictions from biophysical ecological theory for how body temperature should vary with microclimate for 269 lizard populations across open, semi-open, and closed habitats worldwide. We extend existing biophysical models to incorporate canopy shade effects via leaf area index, test whether body temperature varies with canopy density as predicted by theory, and evaluate the extent to which incorporating canopy density improves model performance in heavily-shaded areas.

RESULTS: We find that body temperatures in open habitats, like deserts, vary with air temperature and incident solar radiation as predicted by biophysical equations, but these relationships break down in forests, where body temperatures become unpredictable. Incorporating leaf area index into our models revealed lower body temperatures in more heavily shaded environments, restoring the predictability of body temperature in forests.

CONCLUSIONS: Although biophysical ecological theory can predict ectotherm body temperature in open habitats, like deserts, these relationships decay in closed forests. Models incorporating remotely-sensed data on canopy density improved predictability of body temperatures in these habitats, providing an avenue to incorporate canopy shade effects into predictions of animals' vulnerability to climate change. These results highlight the thermal threat of changes in canopy structure and loss of forest cover for the world's ectotherms.

KEYWORDS

biophysical ecology, body temperature, canopy cover, land cover change, leaf area index, lizards, macrophysiology, operative temperature, remote sensing, thermal ecology

INTRODUCTION

The implications of higher body temperatures in a warming world may be felt across all scales of life, from metabolic rates (Dillon, Wang, Huey, 2010), to organismal behavior (Kearney, Shine, Porter, 2009; Sinervo, 2010), evolutionary fitness (Kingsolver, Diamond, Buckley, 2013), species' distributions (Parmesan et al., 1999), and ecosystem dynamics (Cramer et al., 2001). Warm-adapted species will benefit from hotter conditions, making a wider range of habitats available and encouraging range expansion (Deutsch et al., 2008; Huey et al., 2009; but c.f. Logan, Huynh, Precious, Calsbeek, 2013). In contrast, many species are already operating with slim thermal safety margins, especially in biodiverse tropical environments (Deutsch et al., 2008; Huey et al., 2009; Khaliq, Hof, Prinzinger, Böhning-Gaese, Pfenninger, 2014; Sunday et al., 2014), suggesting that future temperature increases will reduce activity times (Kearney et al., 2009), lower fitness (Kingsolver et al., 2013), and increase the chance of extinction (Sinervo et al., 2010). These effects may be especially severe in closed-canopy forests, where species tend to be cool-adapted (Deutsch et al., 2008; Huey et al., 2009; Sunday, Bates, Dulvy, 2012). The effects of future warming on ectotherm thermal vulnerability are often predicted using biophysical models of heat flux (Deutsch et al., 2008; Kearney et al., 2009; Sinclair et al., 2016), but how well these models actually capture relationships between microclimate and body temperature at the global scale over which predictions are made is largely untested. Furthermore, these models do not currently incorporate the effects of forest canopy shade on body temperatures, limiting their capacity to capture effects of global change on forest-dwelling species.

Predicting the effects of climate warming and variability on organisms relies on understanding the link between environmental conditions and body temperature (T_b). Although ectotherms must gain their heat from the surrounding environment, standard climate variables, like mean annual air temperature, are poor predictors of T_b worldwide (Meiri et al., 2013), not least because long-term climate averages do not accurately reflect the microclimates experienced by individual organisms (Kearney, Isaac, Porter, 2014; Kearney, Shamakhy, et al., 2014). T_b may also deviate from air temperature, even when measured locally, for two reasons. Firstly, by behaviourally thermoregulating, ectotherms can alter their T_b (Bogert, 1949; Huey, 1974; Huey & Slatkin, 1976). Secondly, even for thermoconformers, T_b is not just a function of air temperature, but also depends on the radiation absorbed and emitted by an animal, along with heat transfer via conduction and convection and evaporative water loss (Porter & Gates, 1969; Gates, 1980; Bakken, Santee, Erskine, 1985; Campbell & Norman, 1998). The temperature that a non-thermoregulating animal would reach at equilibrium in a particular environment is known as operative temperature (Bakken et al., 1985).

Shade plays a key role in determining operative temperature and species' thermal vulnerability to climate change. By reducing the amount of solar radiation reaching an animal, shade can make the difference between lethal and favorable body temperatures (Kearney et al., 2009; Sears et al., 2011; Sunday et al., 2014) and alters the relative importance of different microclimate components: in full sun, T_b will be sensitive to the intensity of incoming solar radiation, but in full shade, T_b should track air temperature (Gates, 1980; Campbell & Norman, 1998; Buckley, 2008; Sears, Raskin, Angilletta, 2011). Shade will become increasingly important under future climate change, especially in tropical regions, as animals must increasingly seek out cooler microhabitats to buffer against rising temperatures (Kearney et al., 2009; Sunday et al., 2014). Despite its importance for the thermal future of biodiversity, shade remains a significant challenge for predicting body temperature through space and time. Currently, most models designed to predict operative and body temperatures of animals predict a broad envelope of possible operative temperatures that encompasses full sun and full shade or must assume a specific, spatially invariant, shade level (Kearney et al., 2009; Sunday et al., 2014; Buckley, Ehrenberger, Angilletta, 2015). While shade from topographical features can be modelled directly, provided detailed topographical information is available (Sears et al., 2011), quantitative measures of shade from other sources—such as the forest canopy, which can greatly alter sub-canopy thermal environments (George, Thompson, Faaborg, 2015; Frey et al., 2016; Lenoir, Hattab, Pierre, 2017)—is lacking from most models. Thus, current biophysical models, while effective in open habitats, are likely to break down in forests, where shade is extensive (but not complete), limiting our ability to accurately predict the thermal futures of species inhabiting these biodiverse environments.

In this paper, we extend existing biophysical models of ectotherm body temperature (Gates, 1980; Campbell & Norman, 1998; Buckley, 2008; Sears et al., 2011) to incorporate shade effects of the forest canopy, allowing for more precise predictions of ectotherm body temperature in forested environments using readily available remote sensing data on canopy density. Firstly, we model the expected relationships between body temperature, air temperature, solar radiation, and wind speed, ignoring canopy effects, and predict that model performance will decline across major habitat types with increasing shade levels, from barren lands to forests. Next, we use our extended model to evaluate whether incorporating remote sensing data to capture shade effects can improve model fit in heavily shaded forests.

METHODS

Predicted relationships between body temperature and microclimate

We generated predictions of how body temperature of a non-thermoregulating lizard will vary with microclimate (air temperature, incident solar radiation, and wind speed) in full sun by modelling operative temperature (T_e) using biophysical principles (Gates, 1980; Campbell & Norman, 1998), following Sears et al. (2011) and Buckley (2008):

$$T_e = T_{air} + \frac{R_{solar} + R_{lw} - \varepsilon_s \sigma (T_{air} + 273)^4}{4\sigma (T_{air} + 273)^3 + c_p \left(1.4 + 0.135\sqrt{\frac{v}{d}}\right)} \qquad \text{Eq. 1}$$

where T_{air} is air temperature, R_{solar} is absorbed incoming solar radiation, R_{lw} is absorbed longwave radiation, ε_s is animal emissivity, σ is the Stefan-Boltzmann constant, c_p is the specific heat of air, d is the characteristic dimension of the animal and v is wind speed. The forest canopy will reduce the amount of solar radiation reaching an animal (Campbell & Norman, 1998), thereby lowering body temperature. We modelled the solar radiation incident on an animal as a function of the direct (beam) radiation, diffuse radiation, and the radiation reflected from the ground, following Buckley (2008) and Sears et al. (2011):

$$R_{solar} = \alpha_s \left(F_p S_p + F_d S_d + F_r S_r\right) \qquad \text{Eq. 2}$$

where α_s is the lizard's absorptivity of solar radiation, F_p, F_d, and F_g are view factors between the lizard and direct solar radiation (S_p), diffuse solar radiation (S_d), and reflected solar radiation (S_r), respectively. Direct and diffuse solar radiation are reduced under the forest canopy; we modelled direct solar radiation reaching an animal under the canopy ($S_{p,sub}$) using equations in Campbell and Norman (1998):

$$S_{p,sub} = \omega_p S_p \qquad \text{Eq 3}$$

where ω_p is the proportion of direct solar radiation that makes it through the canopy, which is an exponential function of LAI (Campbell & Norman, 1998):

$$\omega_p = \exp\left(-\sqrt{\alpha_c} K_{b,z} LAI\right) \qquad \text{Eq 4}$$

where α_c is the average absorptivity of the canopy and $K_{b,z}$ is the extinction coefficient for direct solar radiation at zenith angle z. Following Campbell and Norman (1998), we modelled the diffuse solar radiation under the canopy ($S_{d,sub}$) through numerical integration across all zenith angles (z):

$$S_{d,sub} = S_d 2 \int_0^{\frac{\pi}{2}} \exp\left(-\sqrt{\alpha_c} K_{b,z} LAI\right) \sin z \cos z \, dz \qquad \text{Eq 5}$$

The forest canopy also affects the amount of long-wave radiation reaching an animal from above (Webster et al., 2017). In the absence of a canopy, long-wave radiation from the air (L_a) is calculated as (Campbell & Norman, 1998; Buckley, 2008; Sears et al., 2011):

$$L_a = \varepsilon_{ac} \sigma (T_{air} + 273)^4 \qquad \text{Eq 6}$$

where ε_{ac} is clear-sky emissivity. Under a canopy, long-wave radiation ($L_{a,sub}$) comes from the sky and from the canopy, in proportion to the amount of clear sky (Webster, Rutter, Jonas, 2017):

$$L_{a,sub} = V_s L_a + (1 - V_s) \varepsilon_c \sigma (T_{can} + 273)^4 \qquad \text{Eq 7}$$

where T_{can} is canopy temperature, ε_c is canopy emissivity and V_s is a view factor denoting the proportion of long-wave radiation from clear sky. In Eq 4, the proportion of direct solar radiation reaching an animal through the canopy (ω_p) was modelled as a function of LAI (also see Essery, Pomeroy, Ellis, Link, 2008). As ω_p represents the proportion of radiation non-intercepted by the canopy, we derived the proportion of clear sky (Vs) using Equation 4 but assuming black leaves ($\alpha_c^{=1}$):

$$V_s = \exp\left(-K_{b,z} LAI\right) \qquad \text{Eq 8}$$

The forest canopy will also reflect longwave and reflected solar radiation from the substrate back downward, with the process repeating, attenuated by the absorptivity of the canopy and the ground, (Mahat & Tarboton, 2012), but we do not include this process here. We can now rewrite Eq 1 to include the radiation reaching animals below the canopy as:

$$T_{e,sub} = T_{air} + \frac{R_{solar,sub} + R_{lw,sub} - \varepsilon_s \sigma (T_{air} + 273)^4}{4\sigma (T_{air} + 273)^3 + c_p \left(1.4 + 0.135\sqrt{\frac{v}{d}}\right)} \quad \text{Eq 9}$$

We used Eq 9 to model the predicted relationships between T_b and T_{air}, solar radiation, wind speed and LAI. Full model details and parameter values are given in Appendix S1 in Supporting Information. We varied each environmental variable across the range of values observed in our empirical data to generate predictions of the shape of the relationships between each variable and T_b. We modelled the relationships between T_b and T_{air}, solar radiation, and wind speed at five different LAI levels to visualize interactive effects between these variables. We stress that our aim was not to predict the absolute values of T_b in our empirical dataset, but rather the relationships that emerge between T_b, microclimate, and LAI.

Empirical data

We tested whether global relationships between ectotherm body temperature, microclimate and LAI matched those predicted by our biophysical model using a dataset, collected from the literature, of mean body temperatures for 269 diurnal, non-fossorial mainland lizard populations (179 species; Fig. S1.1) sampled between 1990 and 2010, building on an existing database (Clusella-Trullas, Blackburn, Chown, 2011; Meiri et al., 2013). A list of data sources is found in Appendix 1. Following Meiri et al. (2013), we did not set a minimum sample size, pooled data across sexes and life stages, and excluded temperatures or populations sampled at night. We limited our data to post-1990 to limit confounding effects of substantial 20th century land cover change on our estimates of canopy structure (see below). For each population, we extracted the mean daytime (06:00–18:00 local time) air temperature 1cm above ground (averaged across rock, soil, and sand), air temperature at 1.2m, solar radiation, and wind speed at 1cm from the microclim dataset (Kearney, Isaac, et al., 2014) for the sampling months reported for each study. We extracted microclimate data values in full sun for open and semi-open habitats and in full shade for closed forests. We assigned each population to one of these habitat types based on the geographical coordinates reported for a population. While this may not capture microhabitat preferences perfectly (e.g. forest gap or edge specialists), this is likely to add noise to our analysis rather than bias it. We made these assignations (Table S1.2) based on combining categories included in the global land cover consensus product (Tuanmu & Jetz, 2014) and finding the land cover (closed, semi-open, open) with the highest probability of occurring at each location, resulting in 27 closed, 123 semi-open, and 119 open habitat populations (Fig. S1.1).

We determined whether species were ground-dwelling, arboreal or semi-arboreal (use ground and trees, or use shrubs) from the literature, using the source paper for the T_b data where possible and other literature or expert knowledge where necessary. Data sources are given in Appendix 1 and the accompanying dataset. For ground-dwellers, we used air temperature and wind speed at 1cm for all analyses, for arboreal species we used air temperature and wind speed at 1.2m and for semi-arboreal species, we used the average of 1cm and 1.2m. We inferred wind speed at 1.2m using the equations given for this purpose in Kearney, Isaac, et al. (2014). We did not consider variation in substrate temperature because in our empirical dataset (see below), air and soil temperature were highly correlated ($r=0.94$, $P<<0.001$). If sampling months were not reported we used a summer average (northern hemisphere: April–September, southern hemisphere: October–March) instead. For populations whose coordinates fell in the ocean (likely due to georeferencing error), we used conditions from the nearest piece of land, provided it was within 1 grid cell (at 0.1667 x 0.1667 DD resolution) of the original coordinates.

We also extracted leaf area index (LAI) for each population's location. We used the mean of 8-day MODIS reprocessed composites of LAI (Yuan, Dai, Xiao, Ji, Shangguan, 2011) across the sampling months at 30 arc-sec spatial resolution, averaged from 2001-2010. LAI data are freely available from http://globalchange.bnu.edu.cn/research/lai/. There is a partial temporal mismatch between our T_b data

(1990-2010) and our LAI data (2001-2010) that represents a tradeoff between limiting effects of land cover change on LAI estimates for lizard sampling locations and maintaining sample size.

Testing for predicted relationships

We initially fit regression models that excluded LAI and modelled T_b as linear functions of air temperature and solar radiation and quadratic functions of wind speed to approximate the predicted non-linearity in the T_b wind speed relationships (Eqs 1 and 9). Wind speed data were right-skewed, so we fifth-root transformed this variable to reduce high leverage of large values. We did not used a log-transformation to avoid taking the logarithm of zero. We removed non-significant terms from our model sequentially, based on P-value, starting with quadratic terms. Next, we added LAI to our full regression model, including a quadratic term to capture non-linearity, as well as interactions with wind speed and solar radiation. We removed non-significant terms as above, beginning with interactions, then quadratic terms. LAI was also right-skewed so we square-root transformed it to reduce influence of a few large values. We repeated regressions for all data habitats pooled and each habitat (open, semi-open, closed) separately.

We fit all regressions using the lmekin function in the coxme package (Therneau, 2015) in R 3.4.3 (R Core Team, 2018) to simultaneously incorporate spatial and phylogenetic non-independence into our regressions (Freckleton & Jetz, 2009). Based on Tonini, Beard, Ferreira, Jetz, Pyron's (2016) consensus tree, we used shared branch length between species (or populations, see below) as our measure of phylogenetic covariance and the inverse of distance between locations as our spatial covariance matrix. We also considered an alternative phylogenetic covariance structure by transforming the tree using Pagel's λ of T_b and then recalculating shared branch lengths. Where multiple populations of the same species from different locations were included in our data, we replaced a species' terminal branch with a randomly resolved clade whose crown node depth was chosen from a random uniform distribution with a maximum length equal to the original terminal branch. Populations were added to the tree prior to pruning species not included in our analysis and thus are represented as branching events which occurred after a species diverged from its sister. After fitting regressions, we calculated the marginal (R^2_m) and conditional (R^2_c) R^2 values (Nakagawa & Schielzeth, 2013). R^2_m is the proportion of variance explained by environmental variables and R^2_c is the variance explained by environment, space and phylogeny.

Geographical bias

Our T_b data were highly geographically biased toward South America (Fig. S1.1). To determine how this may have affected our results, we randomly sub-sampled the South American data and refit the final model for each habitat type and all habitat types combined. For each regression, we reduced the number of South American data points so that they were equal in number to the next highest continent (Table 1). We repeated this process 1000 times and computed the number of times we detected a significant ($P<0.05$) relationship in the direction matching that found in the original regression. We did not geographically subsample closed habitats because only three populations were not from South America.

RESULTS

Biophysical predictions

The model based on environmental biophysical principles for a non-thermoregulating lizard in full sun (LAI=0); Eq. 9) predicts that T_b will increase linearly with air temperature and solar radiation, and that it will decline proportionally to the inverse of the square root of wind speed (Fig. 1). T_b is predicted to decline in a nearly exponential fashion with increasing LAI (Fig 1) and to have interactive effects on T_b with wind speed and solar radiation, but not air temperature (Fig 2). As LAI increases, solar radiation above the canopy and wind speed both are predicted to have diminishing influence on T_b (Fig. 2).

Microclimate–T_b relationships

As predicted, and after accounting for phylogenetic and spatial autocorrelation, we found positive, global relationships between T_b and air temperature (slope±s.e.=0.21±0.03, $P=6.5\times10^{-10}$, Table S1.3) and T_b and solar radiation (slope±s.e.=0.006±0.003, P=0.02, Table S1.3). Contrary to our prediction, we found no relationship between T_b and wind speed (linear slope±s.e.=-2.6±2.4, P=0.27, Table S1.3). Although relationships with air temperature and solar radiation were significant, these variables explained just 13% of the variance in T_b worldwide (Table S1.3). Regression results using a Pagel's λ transformed tree were nearly identical with no changes in direction of coefficients, R^2_m, or significance (Table S1.4).

As predicted by biophysical models, T_b in open habitats, where there is less extensive shade, was significantly related air temperature and solar radiation (P<0.005 for both; Fig. 3; Table S1.5). We found no relationship with wind speed (P=0.11; Fig. 3; Table S1.5). In total, temperature and solar radiation explained 35% of the variance in T_b (Table S1.5). The variance explained by microclimate declined to 10% in semi-open habitats (Table S1.6), where there was no relationship between T_b and solar radiation or wind speed (P>0.7 for both; Table S1.6), but the significant relationship with air temperature was retained (slope±s.e.=0.18±0.05, P=0.0003, Fig. 3). These relationships did not change when a Pagel's λ-transformed phylogeny was used (Table S.4)

In shade-dominated closed forests, we found no significant relationships between T_b and air temperature, solar radiation, or wind speed (Fig. 3; Table S1.7; P>0.25 in all cases). The low sample size (n=27) in closed forests compared to semi-open (n=123) and open habitats (n=119) results in low statistical power. In closed forests, to achieve significance at P<0.05 with statistical power of 0.8, we would have needed sample sizes of 569 (air temperature), 362 (solar radiation), or 193 (wind speed), suggesting that the lack of relationships in closed forests is not simply a function of lower power compared to open and semi-open habitats. The variance in T_b explained by microclimate including air temperature, solar radiation and a linear wind speed term was only 8% (Table S1.7). These results were insensitive to using a Pagel's λ-transformed phylogeny (Table S4).

LAI and T_b relationships

We found no global relationship between T_b and LAI, either as a main effect or as interactions with solar radiation and wind speed when all land cover types were pooled (P>0.25 in all cases; Fig. 4; Table S1.3). However, as predicted, T_b was negatively related to LAI in closed habitats (Fig. 4; Table S1.3; slope±s.e.=-5.0±0.2.3, P=0.03), We found no significant interactions between LAI and wind speed or solar radiation in these habitats (Table S1.3). Including LAI in regressions of T_b on micro-environmental conditions in closed forests almost tripled the variance explained by microclimate (T_{air}, solar radiation and linear wind speed) alone from 7% to 19% (Fig. 4; Table S1.7). In contrast, LAI explained very little additional variance in T_b in semi-open and open habitats or when all data were pooled (<2%; Fig. 4; Tables S1.3, S1.6, S1.7), signifying it is of little to no importance for T_b in these habitats. None of these regression results were affected by using a Pagel's λ-transformed phylogeny (Table S1.4).

Geographical bias.

Subsampling our South America data revealed that relationships between T_b and air temperature were robust to geographical bias in our dataset (Table 1). Relationships with solar radiation were variable when all habitat types were pooled, but their direction was consistent in open habitats, though only significant 11% of the time (Table 1).

DISCUSSION

We identified a systematic decay in the ability of existing biophysical models to predict global variation in body temperature (T_b) across major habitat types as a function of shade availability, from open habitats where models performed well to closed forests where T_b was unpredictable. Relationships between body temperature, air temperature and solar radiation matched predictions from classic biophysical models in open habitats across the globe, but the same models failed in forests because even estimates of air temperature from full shade fail to accurately capture thermal conditions under the canopy. By extending biophysical models of ectotherm heat flux to incorporate the interception of solar radiation by the forest canopy, we showed it is possible to predict ectotherm body temperature variation in forests using readily available remote sensing data. As predicted by our model, we found that in closed forests, body temperatures cooled with increasing canopy density. Moreover, including LAI in T_b–microclimate regressions almost tripled the variance explained by in closed forests, revealing potential to improve predictions of body temperatures of forest species under future climate change and highlighting the importance of future canopy thinning and loss for the thermal future of forest ectotherms.

The relative importance of different microclimate variables for T_b varied across major habitat types. In open habitats, T_b was sensitive to air temperature and solar radiation, as predicted by biophysical models (Gates, 1980; Campbell & Norman, 1998; Buckley, 2008; Sears et al., 2011). These relationships reflect proximate effects of microclimate on heating and cooling of organisms where shade is too rare or unevenly distributed to permit efficient thermoregulation to lower temperatures (Huey, 1974; Huey & Slatkin, 1976; Sears et al., 2016), but also capture longer-term adaptive responses that have resulted in higher preferred temperatures in open environments, especially if these environments are also drier (Clusella-Trullas et al., 2011). Contrary to biophysical predictions, we found no relationship with wind speed in open habitats which could either reflect lower accuracy of wind data, or perhaps reduced activity of lizards in windier conditions (e.g. Logan, Fernandez, Calsbeek, 2015). The sensitivity of the solar radiation (but not air temperature) relationship to sub-sampling of the South American data indicate that it has a weaker effect than temperature and thus its detectability may be more prone to a loss of statistical power. However, it is also possible that the effects of solar radiation are stronger in South America than elsewhere. *Liolaemus*, which comprise much of our South American data, span exceptionally large elevational and latitudinal gradients gradient (Pincheira-Donoso, Tregenza, Witt, Hodgson, 2013) and thus may experience exceptional variation in solar radiation; this additional variation could make detecting effects of this variable easier in South America than elsewhere.

In semi-open habitats, we found no relationship between T_b and wind speed or solar radiation. In these habitats, sun and shade should both be abundant across the landscape. By shuttling in and out of the sun, thermoregulating individuals can maintain body temperatures at, or close to, preferred levels

(Huey, 1974), decoupling field-active T_b from incident solar radiation. However, despite this potential for thermoregulation, we still found a positive T_b–air temperature relationship, suggesting that even an abundance of thermoregulation opportunities in these habitats cannot completely degrade the influence of air temperature on body temperature at the global scale. Additionally, lizards inhabiting semi-open habitats may have evolved higher preferred or optimal temperatures than closed forest species (Logan et al., 2013), which could also have contributed to the observed relationship between air temperature and T_b in these environments.

In contrast to open habitats, relationships between microclimate variables and T_b in closed habitats (forests) did not match predictions of existing biophysical models. Biophysical principles predict that T_b should track air temperature in full shade, as there is no additional heat input from direct solar radiation (Gates, 1980; Campbell & Norman, 1998). As such, many deep forest species are thermoconformers with cooler preferred temperatures (Huey et al., 2009). Yet, we found no relationship between T_b and air temperature in closed habitats. This discrepancy reflects a limitation of current biophysical models, and global microclimate datasets, to accurately capture thermal conditions for ectotherms in these environments. Currently, such datasets, and the biophysical models that use them, must assume a particular shade value (e.g. 100% shade for a closed forest canopy). However, a portion of incident solar radiation still penetrates a closed canopy (Campbell & Norman, 1998; also see Eqs 3–5), violating the full shade assumption and allowing T_b to deviate from air temperature. Extending biophysical models to include effects of LAI on solar radiation, as we have done, incorporates this additional source of radiation and eliminates the need to assume a particular shade level, allowing for improved predictions of operative temperatures within forests.

Incorporating a remotely-sensed measure of canopy LAI greatly improved the R^2 of our regression models in closed forests, indicating that it does capture valuable additional information on thermal environment which is missing from global microclimate variables. Lizards had cooler body temperatures in forests with denser canopies (higher LAI), as predicted by our extended biophysical model. However, we did not find a curvilinear relationship, as predicted, suggesting that there are additional factors that could be usefully incorporated into our model. For example, arboreality will expose species to different thermal conditions from ground level to the canopy (Bakken, 1989; Scheffers et al., 2013; Spicer et al., 2017). Although we attempted to account for the major temperature differences between ground-dwelling and arboreal lizards, more precise data on perch height and type could improve predictions of T_b in treed environments. Also, our model did not include long-wave radiation from the ground that may have been reflected back downwards toward the animal by the canopy (Mahat & Tarboton, 2012), surface conduction; or variation in latent heat loss. Another possibility is that our results reflect both proximate effects of LAI on forest-lizard T_b and adaptive outcomes of living in these environments as sub-canopy lizards in cooler, closed, environments have adapted to prefer, and function at, lower body temperatures (Ruibal, 1961; Hertz, 1974; Huey et al., 2009; Munoz et al., 2016). The increase in T_b as LAI decreased is consistent with more solar radiation reaching sub-canopy microenvironments, raising sub-canopy temperatures (Hardwick et al., 2015) and allowing for opportunistic thermoregulation to higher T_b (Otero, Huey, Gorman, 2015), which would permit the occurrence of species adapted to warmer thermal conditions in gaps and edges (Ruibal, 1961; Munoz et al., 2016).

The reliance of T_b on canopy density in forests highlights the thermal threat of land use and canopy change for ectotherms. Previous biophysical modelling efforts at broad scales have predicted that in a warming world, shade will become increasingly important for ectotherms (Kearney et al., 2009; Sunday et al., 2014), Our results provide empirical evidence of the effect of canopy-shade on body temperature at the scale of these modelled predictions, suggesting that canopy loss would reduce the buffering capacity of shaded environments, further raising body temperatures. In addition to wholesale canopy loss, more subtle changes in canopy density could also raise T_b and narrow thermal safety margins for forest ectotherms, as well as open new opportunities for more warm-adapted species (Huey et al., 2009; but c.f. Logan et al., 2013). In tropical forests, drought causes increased tree mortality along with losses of water content, photosynthetic activity (greenness), and canopy volume (Phillips et al., 2010; Xu et al., 2011; Saatchi et al., 2013; Zhou et al., 2014), leading to increases in the light incident to the forest floor (Slik, 2004). Thus, the increases in drought intensity and/or frequency predicted by global climate models (Dai, 2013; Trenberth et al., 2014) will have indirect effects on T_b via alterations in canopy density, reducing thermal safety margins and the potential for vegetation shade to act as thermal microrefugia (Lenoir et al., 2017) as global temperatures continue to rise. These potential indirect effects of drought highlight the importance of precipitation dynamics, and not just air temperature, for ectotherm thermal niches (Clusella-Trullas et al., 2011).

Even the relatively coarse-grained, satellite-derived, LAI product used here tripled the fit of T_b–microclimate models in forests, capturing the importance of shade for ectotherms in these environments. At narrower spatial extents, the potential for remote sensing to improve understanding of shade variation and predict thermal habitat quality is even greater. Remote sensing using LiDAR and hyperspectral sensors on airborne platforms capture variation in canopy and sub-canopy vegetation structure at centimeter scales and thus can provide information at scales relevant to individual organisms' movement (George et al., 2015; Frey et al., 2016; Lenoir et al., 2017), and potentially allow for precise estimates of an individual organism's exposure to sun. These products can not only capture the total shade available, but also its spatial configuration, which can have important implications for thermoregulation (Sears & Angilletta, 2015; Sears et al., 2016). Remote sensing data can also improve temporal resolution of predictions of thermal vulnerability in response to land cover change and drought dynamics. Even at the coarser spatial resolutions used here, we have found that canopy structure leaves a predictable signature on lizard body temperatures across the globe, demonstrating the potential of remote sensing products, when properly calibrated, to narrow the predictive envelope of purely biophysical models and provide more precise predictions of T_b in free-living ectotherms across broad spatial extents. Moreover, the sensitivity of T_b to canopy density suggests that changes in forest cover, whether from wholesale land cover change or more subtle alterations of canopy structure, may intensify the thermal challenges faced by organisms in the Anthropocene.

REFERENCES

Bakken, G.S. (1989) Arboreal perch properties and the operative temperature experienced by small animals. *Ecology*, **70**, 922–930.

Bakken, G.S., Santee, W.R. & Erskine, D.J. (1985) Operative and standard operative temperature: Tools for thermal energetics studies. *Integrative and Comparative Biology*, **25**, 933–943.

Bogert, C. (1949) Thermoregulation in reptiles, a factor in evolution. *Evolution*, **3**, 195–211.

Buckley, L.B. (2008) Linking traits to energetics and population dynamics to predict lizard ranges in changing environments. *The American Naturalist*, **171**, E1–E19.

Buckley, L.B., Ehrenberger, J.C. & Angilletta, M.J. (2015) Thermoregulatory behaviour limits local adaptation of thermal niches and confers sensitivity to climate change. *Functional Ecology*, **29**, 1038–1047.

Campbell, G.S. & Norman, J.M. (1998) *An introduction to environmental biophysics*, 2nd edn. Springer-Verlag, New York.

Clusella-Trullas, S., Blackburn, T.M. & Chown, S.L. (2011) Climatic predictors of temperature performance curve parameters in ectotherms imply complex responses to climate change. *The American Naturalist*, **177**, 738–51.

Cramer, W., Bondeau, A., Woodward, F.I., Prentice, I.C., Betts, R.A., Brovkin, V., …, Young-Molling, C. (2001) Global response of terrestrial ecosystem structure and function to CO2 and climate change: results from six dynamic global vegetation models. *Global Change Biology*, **7**, 357–373.

Dai, A.G. (2013) Increasing drought under global warming in observations and models. *Nature Climate Change*, **3**, 52–58.

Deutsch, C.A., Tewksbury, J.J., Huey, R.B., Sheldon, K.S., Ghalambor, C.K., Haak, D.C. & Martin, P.R. (2008) Impacts of climate warming on terrestrial ectotherms across latitude. *Proceedings of the National Academy of Sciences of the United States of America*, **105**, 6668–6672.

Dillon, M.E., Wang, G. & Huey, R.B. (2010) Global metabolic impacts of recent climate warming. *Nature*, **467**, 704–706.

Essery, R., Pomeroy, J., Ellis, C. & Link, T. (2008) Modelling longwave radiation to snow beneath forest canopies using hemispherical photography or linear regression. *Hydrological Processes*,

22, 2788–2800.
Freckleton, R.P. & Jetz, W. (2009) Space versus phylogeny: disentangling phylogenetic and spatial signals in comparative data. *Proceedings of the Royal Society B - Biological Sciences*, **276**, 21–30.
Frey, S.J.K., Hadley, A.S., Johnson, S.L., Schulze, M., Jones, J.A. & Betts, M.G. (2016) Spatial models reveal the microclimatic buffering capacity of old-growth forests. *Science Advances*, **2**, e1501392.
Gates, D.M. (1980) *Biophysical Ecology*, Springer-Verlag, New York.
George, A.D., Thompson, F.R. & Faaborg, J. (2015) Using LiDAR and remote microclimate loggers to downscale near-surface air temperatures for site-level studies. *Remote Sensing Letters*, **6**, 924–932.
Hardwick, S.R., Toumi, R., Pfeifer, M., Turner, E.C., Nilus, R. & Ewers, R.M. (2015) The relationship between leaf area index and microclimate in tropical forest and oil palm plantation: Forest disturbance drives changes in microclimate. *Agricultural and Forest Meteorology*, **201**, 187–195.
Hertz, P.E. (1974) Thermal passivity of a tropical forest lizard, *Anolis polylepis*. *Journal of Herpetology*, **8**, 323–327.
Huey, R.B. (1974) Behavioral thermoregulation in lizards: importance of associated costs. *Science*, **184**, 1001–1003.
Huey, R.B., Deutsch, C.A., Tewksbury, J.J., Vitt, L.J., Hertz, P.E., Alvarez Pérez, H.J. & Garland, T. (2009) Why tropical forest lizards are vulnerable to climate warming. *Proceedings of the Royal Society B - Biological Sciences*, **276**, 1939–1948.
Huey, R.B. & Slatkin, M. (1976) Cost and benefits of lizard thermoregulation. *The Quarterly Review of Biology*, **51**, 363–384.
Kearney, M., Shine, R. & Porter, W.P. (2009) The potential for behavioral thermoregulation to buffer “cold-blooded” animals against climate warming. *Proceedings of the National Academy of Sciences of the United States of America*, **106**, 3835–3840.
Kearney, M.R., Isaac, A.P. & Porter, W.P. (2014a) microclim: Global estimates of hourly

microclimate based on long-term monthly climate averages. *Scientific Data*, **1**, 140006.

Kearney, M.R., Shamakhy, A., Tingley, R., Karoly, D.J., Hoffmann, A.A., Briggs, P.R. & Porter, W.P. (2014b) Microclimate modelling at macro scales: a test of a general microclimate model integrated with gridded continental-scale soil and weather data. *Methods in Ecology and Evolution*, **5**, 273–286.

Khaliq, I., Hof, C., Prinzinger, R., Böhning-Gaese, K. & Pfenninger, M. (2014) Global variation in thermal tolerances and vulnerability of endotherms to climate change. *Proceedings of the Royal Society B - Biological Sciences*, **281**, 20141097.

Kingsolver, J.G., Diamond, S.E. & Buckley, L.B. (2013) Heat stress and the fitness consequences of climate change for terrestrial ectotherms. *Functional Ecology*, **27**, 1415–1423.

Lenoir, J., Hattab, T. & Pierre, G. (2017) Climatic microrefugia under anthropogenic climate change: implications for species redistribution. *Ecography*, **40**, 253–266.

Logan, M.L., Fernandez, S.G. & Calsbeek, R. (2015) Abiotic constraints on the activity of tropical lizards. *Functional Ecology*, **29**, 694–700.

Logan, M.L., Huynh, R.K., Precious, R.A. & Calsbeek, R.G. (2013) The impact of climate change measured at relevant spatial scales: new hope for tropical lizards. *Global Change Biology*, **19**, 3093–3102.

Mahat, V. & Tarboton, D.G. (2012) Canopy radiation transmission for an energy balance snowmelt model. *Water Resources Research*, **48**, W01534.

Meiri, S., Bauer, A.M., Chirio, L., Colli, G.R., Das, I., Doan, T.M., …, Van Damme, R. (2013) Are lizards feeling the heat? A tale of ecology and evolution under two temperatures. *Global Ecology and Biogeography*, **22**, 834–845.

Munoz, M.M., Langham, G.M., Brandley, M.C., Rosauer, D.F., Williams, S.E. & Moritz, C. (2016) Basking behavior predicts the evolution of heat tolerance in Australian rainforest lizards. *Evolution*, **70**, 2537–2549.

Nakagawa, S. & Schielzeth, H. (2013) A general and simple method for obtaining R^2 from generalized linear mixed-effects models. *Methods in Ecology and Evolution*, **4**, 133–142.

Otero, L.M., Huey, R.B. & Gorman, G.C. (2015) A few meters matter: Local habitats drive reproductive cycles in a tropical lizard. *The American Naturalist*, **186**, E72--80.

Parmesan, C., Ryrholm, N., Stefanescu, C., Hill, J.K., Thomas, C.D., Descimon, H., …, Warren, M. (1999) Poleward shifts in geographical ranges of butterfly species associated with regional warming. *Nature*, **399**, 579–583.

Phillips, O.L., van der Heijden, G., Lewis, S.L., López-González, G., Aragão, L.E.O.C., Lloyd, J., …, Vilanova, E. (2010) Drought-mortality relationships for tropical forests. *New Phytologist*, **187**, 631–646.

Pincheira-Donoso, D., Tregenza, T., Witt, M.J. & Hodgson, D.J. (2013) The evolution of viviparity opens opportunities for lizard radiation but drives it into a climatic cul-de-sac. *Global Ecology and Biogeography*, **22**, 857–867.

Porter, W. & Gates, D. (1969) Thermodynamic equilibria of animals with environment. *Ecological Monographs*, **39**, 227–244.

R Core Team (2018) R: A Language and Environment for Statistical Computing. v3.4.4. http://www.r-project.org.

Ruibal, R. (1961) Thermal relations of five species of tropical lizards. *Evolution*, **15**, 98–111.

Saatchi, S., Asefi-Najafabady, S., Malhi, Y., Aragão, L.E.O.C., Anderson, L.O., Myneni, R.B. & Nemani, R. (2013) Persistent effects of a severe drought on Amazonian forest canopy. *Proceedings of the National Academy of Sciences of the United States of America*, **110**, 565–570.

Scheffers, B.R., Phillips, B.L., Laurance, W.F., Sodhi, N.S., Diesmos, A. & Williams, S.E. (2013) Increasing arboreality with altitude: a novel biogeographic dimension. *Proceedings of the Royal Society B - Biological Sciences*, **280**, 20131581.

Sears, M.W. & Angilletta, M.J. (2015) Costs and benefits of thermoregulation revisited: both the heterogeneity and spatial structure of temperature drive energetic costs. *The American Naturalist*, **185**, E94–E102.

Sears, M.W., Angilletta, M.J., Schuler, M.S., Borchert, J., Dilliplane, K.F., Stegman, M., …, Mitchell, W.A. (2016) Configuration of the thermal landscape determines thermoregulatory performance of ectotherms. *Proceedings of the National Academy of Sciences of the United States of*

America, **113**, 10595–600.

Sears, M.W., Raskin, E. & Angilletta, M.J. (2011) The world is not flat: Defining relevant thermal landscapes in the context of climate change. *Integrative and Comparative Biology*, **51**, 666–675.

Sinclair, B.J., Marshall, K.E., Sewell, M.A., Levesque, D.L., Willett, C.S., Slotsbo, S., …, Huey, R.B. (2016) Can we predict ectotherm responses to climate change using thermal performance curves and body temperatures? *Ecology Letters*, **19**, 1372–1385.

Sinervo, B., Mendez-de-la-Cruz, F., Miles, D.B., Heulin, B., Bastiaans, E., Cruz, M.V.S., …, Sites, J.W. (2010) Erosion of lizard diversity by climate change and altered thermal niches. *Science*, **328**, 894–899.

Slik, J.W.F. (2004) El Niño droughts and their effects on tree species composition and diversity in tropical rain forests. *Oecologia*, **141**, 114–120.

Spicer, M.E., Stark, A.Y., Adams, B.J., Kneale, R., Kaspari, M. & Yanoviak, S.P. (2017) Thermal constraints on foraging of tropical canopy ants. *Oecologia*, **183**, 1007–1017.

Sunday, J.M., Bates, A.E. & Dulvy, N.K. (2012) Thermal tolerance and the global redistribution of animals. *Nature Climate Change*, **2**, 686–690.

Sunday, J.M., Bates, A.E., Kearney, M.R., Colwell, R.K., Dulvy, N.K., …, Huey, R.B. (2014) Thermal-safety margins and the necessity of thermoregulatory behavior across latitude and elevation. *Proceedings of the National Academy of Sciences of the United States of America*, **111**, 5610–5615.

Therneau, T.M. (2015) coxme: mixed effects Cox models. R package version 2.2-7. https://CRAN.R-project.org/package=coxme.

Tonini, J.F.R., Beard, K.H., Ferreira, R.B., Jetz, W. & Pyron, R.A. (2016) Fully-sampled phylogenies of squamates reveal evolutionary patterns in threat status. *Biological Conservation*, **204**, 23–31.

Trenberth, K.E., Dai, A., van der Schrier, G., Jones, P.D., Barichivich, J., Briffa, K.R. & Sheffield, J. (2014) Global warming and changes in drought. *Nature Clim. Change*, **4**, 17–22.

Tuanmu, M.N. & Jetz, W. (2014) A global 1-km consensus land-cover product for biodiversity and ecosystem modelling. *Global Ecology and Biogeography*, **23**, 1031–1045.

Webster, C., Rutter, N. & Jonas, T. (2017) Improving representation of canopy temperatures for modeling subcanopy incoming longwave radiation to the snow surface. *Journal of Geophysical Research: Atmospheres*, **122**, 9154–9172.

Xu, L., Samanta, A., Costa, M.H., Ganguly, S., Nemani, R.R. & Myneni, R.B. (2011) Widespread decline in greenness of Amazonian vegetation due to the 2010 drought. *Geophysical Research Letters*, **38**, L07402.

Yuan, H., Dai, Y., Xiao, Z., Ji, D. & Shangguan, W. (2011) Reprocessing the MODIS Leaf Area Index products for land surface and climate modelling. *Remote Sensing of Environment*, **115**, 1171–1187.

Zhou, L., Tian, Y., Myneni, R.B., Ciais, P., Saatchi, S., Liu, Y.Y., …, Hwang, T. (2014) Widespread decline of Congo rainforest greenness in the past decade. *Nature*, **508**, 86–90.

DATA ACCESSIBILITY

All data used in these analyses will be deposited in FigShare or Dryad upon manuscript acceptance.

Table 1. Consistency of final regression results after randomly sub-setting South American data. N is the number of South American points retained and is equal to the maximum number of points from any other continent. Subsampling and regressions were repeated 1000 times. Sub-setting was not done for closed habitats as only 3 points were outside South America. Columns show the number of regressions coefficients—out of 1000—that matched the sign of the regression on all data, the number of regressions with a significant ($P<0.05$) coefficient and the means and standard deviations (s.d.) of R^2_m and R^2_c. R^2_m (marginal R^2) is the variance explained by predictors and R^2_c (conditional R^2) is the variance explained by predictors, space and phylogeny. T_b is body temperature, Tair is air temperature, SOL is solar radiation, and LAI is the square root of leaf area index.

		Tair		**SOL**		**R^2_m**		**R^2_c**		
Habitat	**Model**	**+**	**P<0.05**	**+**	**P<0.05**	**mean**	**s.d.**	**mean**	**s.d.**	**N**
All	**T_b~Tair +SOL**	1000	1000	447	2	0.16	0.04	0.45	0.26	28
Semi	**T_b~ Tair**	1000	810			0.08	0.04	0.39	0.33	20
Open	**T_b~Tair +SOL+WS**	1000	1000	970	113	0.40	0.06	0.57	0.18	11

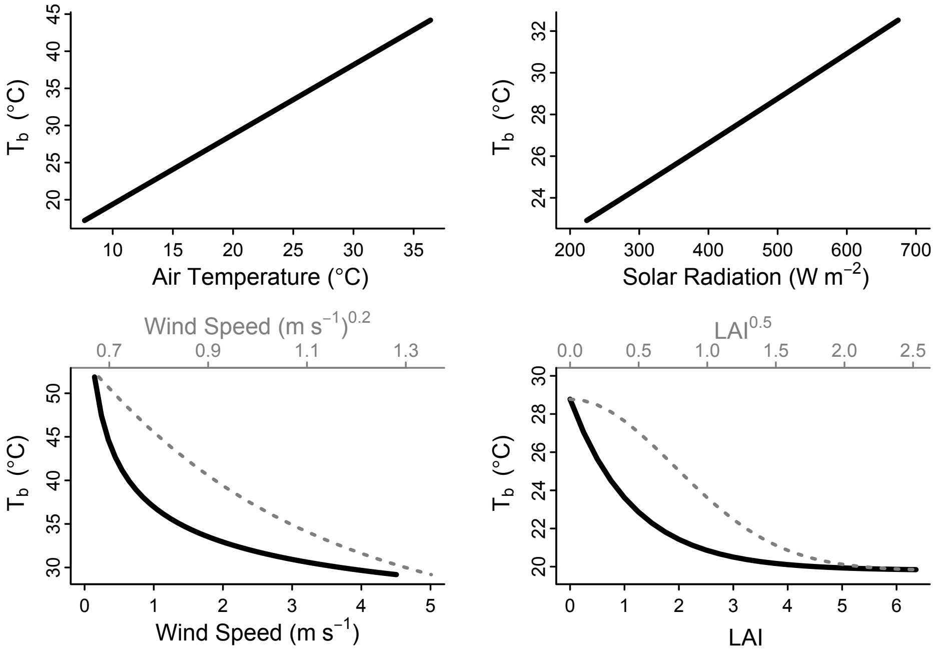

Fig. 1. Predicted relationships between body temperature (T_b), microclimate, and leaf area index (LAI). Predictions are based on a biophysical model of body temperature for a non-thermoregulating lizard (Eq. 9). Parameters for model predictions are given in Appendix 1 and Table S1.1. Relationships with air temperature, solar radiation and wind speed were modelled in full sun (LAI=0). The grey axes and lines for wind speed and LAI show predicted relationships after a fifth root transformation of wind speed and a square root transformation of LAI to allow comparison with patterns in Fig. 4.

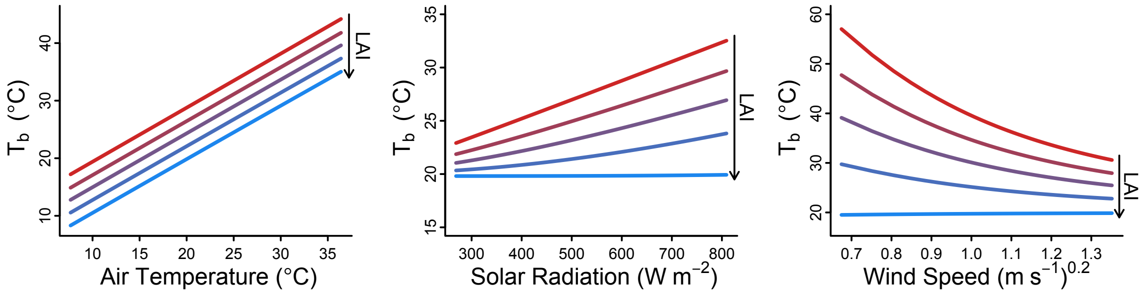

Fig. 2. Predicted effect of LAI on the body temperature (T_b) – microclimate relationship for a non-thermoregulating lizard at equilibrium with its environment. The arrows depict direction of increasing LAI, from low (red) to high (blue). Relationships were modelled using Eq. 9 and all parameters are given in Appendix S1 and Table S1.1. LAI is predicted to have an interactive effect on T_b with solar radiation and wind speed but not air temperature.

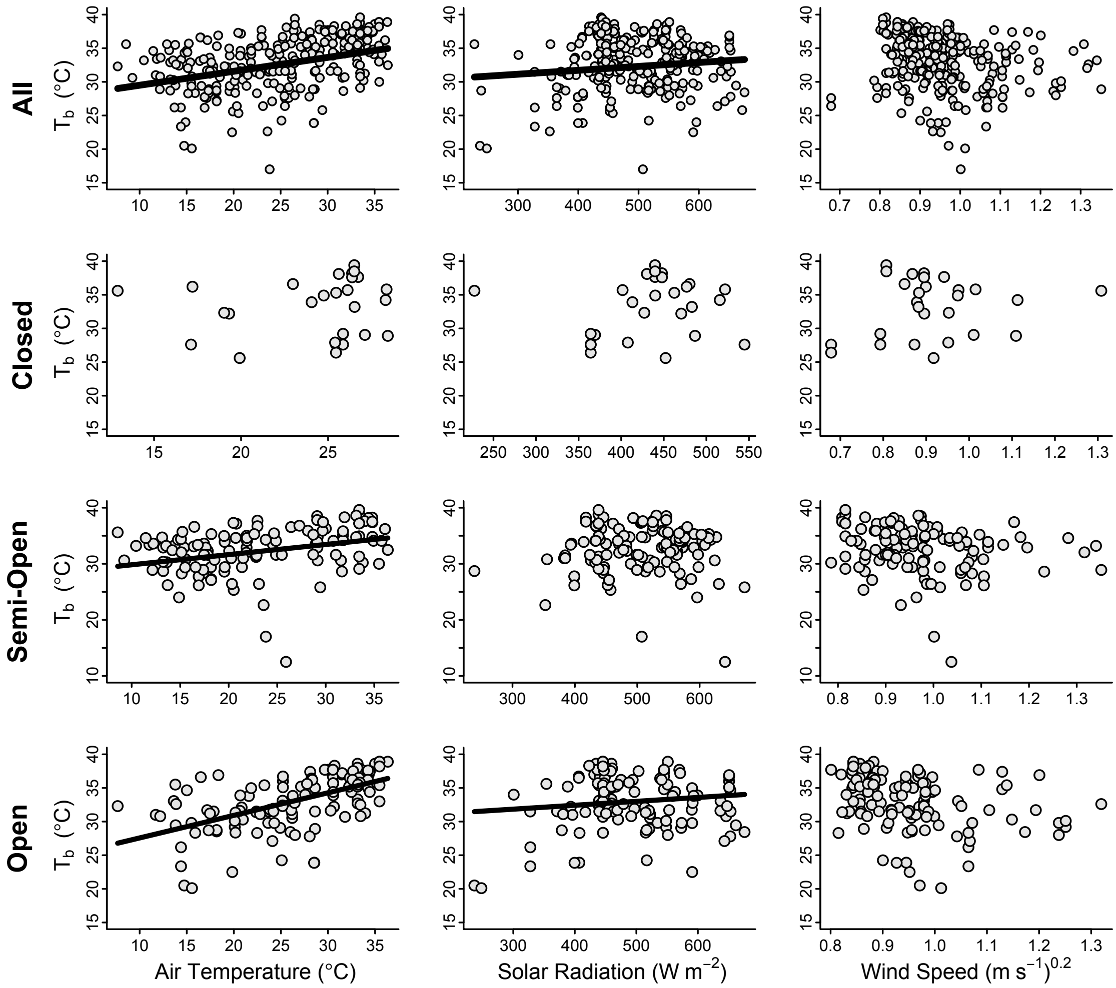

Fig. 3. Relationship between body temperature (T_b) and microclimate for lizards in all habitats and divided by major habitat types that vary in shade availability. Microclimate conditions are daytime averages across the months of T_b collection. Significant ($P<0.05$) relationships after accounting for spatial and phylogenetic relationships are shown as black regression lines. The variance in T_b explained by microclimate (with linear wind speed) was lowest in closed (0.07%, n=27) and semi-open habitats (11%, n=123), highest in open habitats (36%, n=119), and low in the combined data (0.13, n=269). Wind speed was fifth root transformed to reduce skew and leverage of extreme points.

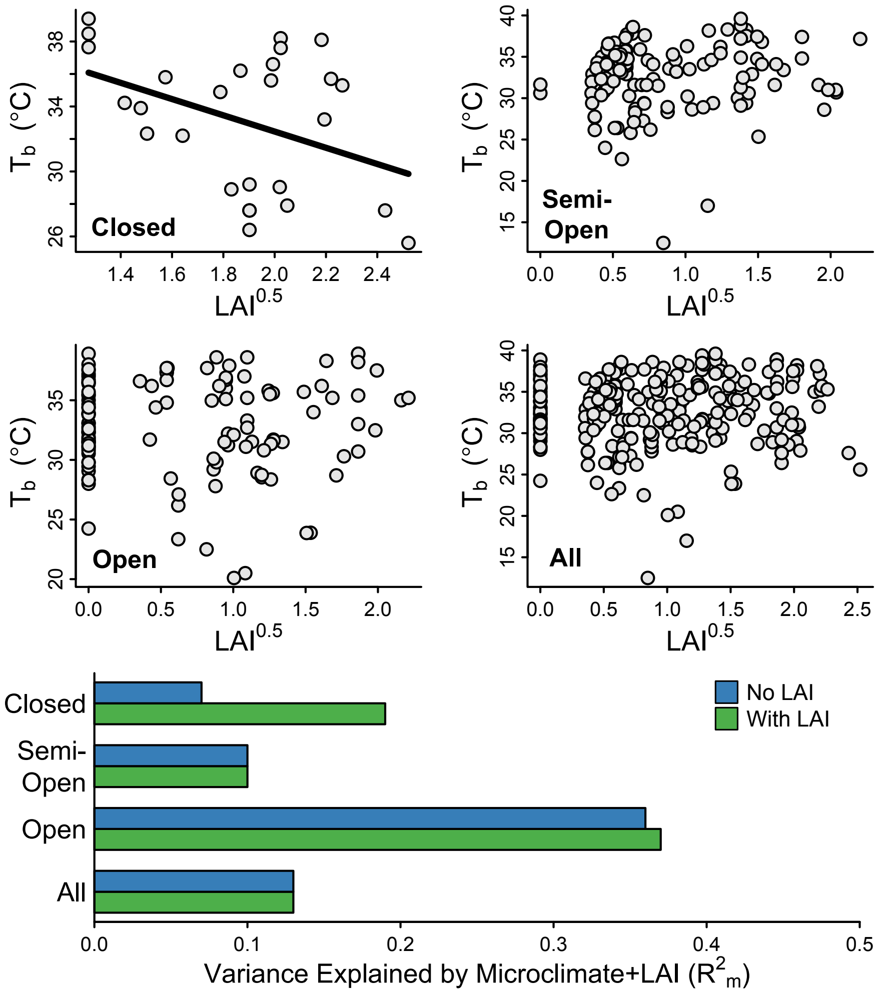

Fig. 4. Relationship between lizard body temperature (T_b) and leaf area index (LAI) in closed, semi-open, and open habitats and all habitats pooled. The relationship was significant (P=0.03) in closed (forest) habitats and was in the direction (negative) predicted by theory, though not curvilinear (see Fig. 1). The bottom panel shows the unique variance explained by environment predictors (marginal R^2) without and with LAI. LAI had little effect on model fit apart from in closed forests.

APPENDIX 1 – Data Sources

Anaya-Rojas, J.M., Serrano-Cardozo, V.H. & Ramirez-Pinilla, M.P. (2010) Diet, microhabitat use, and thermal preferences of *Ptychoglossus bicolor* (Squamata: Gymnophthalmidae) in an organic coffee shade plantation in Colombia. *Papeis Avulsos de Zoologia*, **50**, 159–166.

Andrews, R.M. (2008) Lizards in the slow lane: Thermal biology of chameleons. *Journal of Thermal Biology*, **33**, 57–61.

Andrews, R.M., Mendez-de la Cruz, F.R., Villagran-Santa Cruz, M. & Rodriguez-Romero, F. (1999) Field and selected body temperatures of the lizards *Sceloporus aeneus* and *Sceloporus bicanthalis*. *Journal of Herpetology*, **33**, 93–100.

Ariani, C. V., Menezes, V.A., Vrcibradic, D. & Rocha, C.F.D. (2011) An unusual ecology among whiptails: the case of *Cnemidophorus lacertoides* from a restinga habitat in southern Brazil. *Journal of Natural History*, **45**, 2605–625.

Bashey, F.B. & Dunham, A.E. (1997) Elevational variation in the thermal constraints and microhabitat preferences of the greater earless lizard *Cophosaurus texanus*. *Copeia*, **1997**, 725–737.

Bauwens, D., Castilla, A.M. & Mouton, P.L.F.N. (1999) Field body temperatures, activity levels and opportunities for thermoregulation in an extreme microhabitat specialist, the girdled lizard (*Cordylus macropholis*). *Journal of Zoology*, **249**, 11–18.

Bennett, A.F. (2004) Thermoregulation in African chameleons. *International Congress Series*, **1275**, 234–241.

Bergallo, H.G. & Rocha, C.F.D. (1993) Activity patterns and body temperatures of two sympatric lizards (*Tropidurus torquatus* and *Cnemidophorus ocellifer*) with different foraging tactics in southeastern Brazil. *Amphibia-Reptilia*, **14**, 312–315.

Bujes, C.S. & Verrastro, L. (2006) Thermal biology of *Liolaemus occipitalis* (Squamata, Tropiduridae) in the coastal sand dunes of Río Grande Do Sul, Brazil. *Brazilian Journal of Biology*, **66**, 945–954.

Bustos Zagal, M.G., Manjarrez, J. & Castro-Franco, R. (2013) Uso de microhábitat y termorregulación en *Sceloporus horridus horridus* (Wiegmann 1939) (Sauria: Phrynosomatidae). *Acta Zoológica Mexicana*, **29**, 153–163.

Carothers, J.H., Marquet, P.A. & Jaksic, F.M. (1998) Thermal ecology of a *Liolaemus* assemblage along an Andean altitudinal gradient in Chile. *Revista Chilena de Historia Natural*, **71**, 39–50.

Christian, K.A. & Bedford, G.S. (1995) Seasonal changes in thermoregulation by the frillneck lizard, *Chlamydosaurus kingii*, in tropical Australia. *Ecology*, **76**, 124–132.

Christian, K.A. & Bedford, G.S. (1996) Thermoregulation by the spotted tree monitor, *Varanus scalaris*, in the seasonal tropics of Australia. *Journal of Thermal Biology*, **21**, 67–73.

Christian, K.A. & Weavers, B.W. (1996) Thermoregulation of monitor lizards in Australia: an evaluation of methods in thermal biology. *Ecological Monographs*, **66**, 139–157.

Clemann, N., Melville, J., Ananjeva, N.B., Scroggie, M.P., Milto, K. & Kreuzberg, E. (2008) Microhabitat occupation and functional morphology of four species of sympatric agamid lizards in the Kyzylkum Desert, central Uzbekistan. *Animal Biodiversity and Conservation*, **31**, 51–62.

Clusella-Trullas, S., Van Wyk, J.H. & Spotila, J.R. (2009) Thermal benefits of melanism in cordylid lizards: A theoretical and field test. *Ecology*, **90**, 2297–2312.

Collar, D.C., Schulte, J.A. & Losos, J.B. (2011) Evolution of extreme body aize disparity in monitor lizards (*Varanus*). *Evolution*, **65**, 2664–2680.

Colli, G.R., Caldwell, J.P., Costa, G.C., Gainsbury, A.M., Garda, A.A., Mesquita, D.M., Filho, C.M.M.R., Soares, A.H.B., Silva, V.N., Valdujo, P.H., Vieira, G.H.C., Vitt, L.J., Werneck, F.P., Wiederhecker, H.C. & Zatz, M.G. (2003a) A new species of *Cnemidophorus* (Squamata, Teiidae) from the cerrado biome in central Brazil. *Occasional Papers of the Sam Noble Oklahoma Museum of Natural History*, **14**, 1–14.

Colli, G.R., Giugliano, L.G., Mesquita, D.O. & França, F.G.R. (2009) A new species of *Cnemidophorus* from the Jalapão Region, in the Central Brazilian Cerrado. *Herpetologica*, **65**, 311–327.

Colli, G.R., Mesquita, D.O., Rodrigues, P.V. V. & Kitayama, K. (2003b) Ecology of the gecko *Gymnodactylus geckoides amarali* in a neotropical Savanna. *Journal of Herpetology*, **37**, 694–706.

Contreras-Lozano, J. A., Lazcano, D. & Contreras-Balderas, A.J. (2010) *Barisia ciliaris* (Northern Imbricate Alligator Lizard). Antipredator behavior. *Herpetological Review*, **41**, 217.

Cruz, F.B. (1998) Natural history of *Tropidurus spinulosus* (Squamata: Tropiduridae) from the dry chaco of Salta, Argentina. *Herpetological Journal*, **8**, 107–110.

Cruz, F.B., Belver, L., Acosta, J.C., Villavicencio, H.J., Blanco, G. & Canovas, M.G. (2009) Thermal biology of *Phymaturus* lizards: evolutionary constraints or lack of environmental variation? *Zoology*, **112**, 425–432.

Cruz, F.B., Silva, S. & Scrocchi, G.J. (1998) Ecology of the lizard *Tropidurus etheridgei* (Squamata: Tropidurudae) from the dry Chaco of Salta, Argentina. *Herpetological Natural History*, **6**, 23–31.

Dias, E.J.R. & Rocha, C.F.D. (2004) Thermal ecology, activity patterns, and microhabitat use by two sympatric whiptail lizards (*Cnemidophorus abaetensis* and *Cnemidophorus ocellifer*) from northeastern Brazil. *Journal of Herpetology*, **38**, 586–588.

Dixon, J.R. & Staton, M.A. (1977) Arboreality in the teiid lizard *Cnemidophorus lemniscatus* (Reptilia, Lacertilia, Teiidae) in the Venezuelan Llanos. *Journal of Herpetology*, **11**, 108–111.

Espinoza, R.E., Wiens, J.J. & Tracy, C.R. (2004) Recurrent evolution of herbivory in small, cold-climate lizards: Breaking the ecophysiological rules of reptilian herbivory. *Proceedings of the National Academy of Sciences*, **101**, 16819–16824.

Fuentes, E.R. (1976) Ecological convergence of lizard communities in Chile and California. *Ecology*,

57, 3–17.

Gadsden, H. and J.L.E. (2007) Ecology of the spiny lizard *Sceloporus jarrovii* in the central Chihuahuan Desert. *The Southwestern Naturalist*, **52**, 600–608.

Gandolfi, S.M. & Rocha, C.F.D. (1998) Orientation of thermoregulating *Tropidurus torquatus* (Sauria: Tropiduridae) on termite mounds in an open area of south–eastern Brazil. *Amphibia-Reptilia*, **19**, 319–323.

Grismer, L.L. (2011) *Lizards of Peninsular Malaysia, Singapore and Their Adjacent Archipelagos*, Edition Chimaira.

Guizado-Rodriguez, A., Garcia-Vazquez, U.O. & Solano-Zavaleta, I. (2011) Thermoregulation by a population of *Sceloporus palaciosi* from Sierra del Ajusco, Distrito Federal, Mexico. *The Southwestern Naturalist*, **56**, 120–124.

Gutierrez, J.A., Krenz, J.D. & Ibarguengoytia, N.R. (2010) Effect of altitude on thermal responses of *Liolaemus pictus argentinus* in Argentina. *Journal of Thermal Biology*, **35**, 332–337.

Gvozdik, L. (2002) To heat or to save time? Thermoregulation in the lizard *Zootoca vivipara* (Squamata: Lacertidae) in different thermal environments along an altitudinal gradient. *Canadian Journal of Zoology-Revue Canadienne De Zoologie*, **80**, 479–492.

Hatano, F.H., Vrcibradic, D., Galdino, C.A.B., Cunha-Barros, M., Rocha, C.F.D. & Van Sluys, M. (2001) Thermal ecology and activity patterns of the lizard community of the restinga of Jurubatiba, Macaé, RJ. *Revista Brasileira de Biologia*, **61**, 287–294.

Herrel, A., Meyers, J.J. & Vanhooydonck, B. (2002) Relations between microhabitat use and limb shape in phrynosomatid lizards. *Biological Journal of the Linnean Society*, **77**, 149–163.

Ibarguengoytia, N.R. (2005) Field, selected body temperature and thermal tolerance of the syntopic lizards *Phymaturus patagonicus* and *Liolaemus elongatus* (Iguania: Liolaemidae). *Journal of Arid Environments*, **62**, 435–448.

Ibarguengoytia, N.R., Ascota, J.C., Boretto, J.M., Villavicencio, H.J., Marinero, J.A. & Krenz, J.D. (2008) Field thermal biology in *Phymaturus* lizards: comparisons from the Andes to the Patagonian steppe in Argentina. *Journal of Arid Environments*, **72**, 1620–1630.

Ibarguengoytia, N.R. & Cussac, V.E. (2002) Body temperatures of two viviparous *Liolaemus* lizard species, in Patagonian rain forest. *Herpetological Journal*, **12**, 131–134.

Ibarguengoytia, N.R., Medina, S.M., Fernandez, J.B., Gutierrez, J.A., Tappari, F. & Scolaro, A. (2010) Thermal biology of the southernmost lizards in the world: *Liolaemus sarmientoi* and *Liolaemus magellanicus* from Patagonia, Argentina. *Journal of Thermal Biology*, **35**, 21–27.

Jaksić, F.M., Núnez, H. & Ojeda, F.P. (1980) Body proportions, microhabitat selection, and adaptive radiation of *Liolaemus* lizards in central Chile. *Oecologia*, **45**, 178–181.

Kiefer, M.C., Van Sluys, M. & Rocha, C.F.D. (2005) Body temperatures of *Tropidurus torquatus* (Squamata, Tropiduridae) from coastal populations: do body temperatures vary along their geographic range? *Journal of Thermal Biology*, **30**, 449–456.

Koenig, J., Shine, R. & Shea, G. (2001) The ecology of an Australian reptile icon: how do blue-tongued lizards (*Tiliqua scincoides*) survive in suburbia? *Wildlife Research*, **28**, 215–227.

Labra, A. (1995) Thermoregulation in *Pristidactylus* lizards (Polycridae): effects of group size. *Journal of Herpetology*, **29**, 260–264.

Labra, A. & Bozinovic, F. (2002) Interplay between pregnancy and physiological thermoregulation in *Liolaemus* lizards. *Ecoscience*, **9**, 421–426.

Labra, A., Pienaar, J. & Hansen, T.F. (2009) Evolution of thermal physiology in *Liolaemus* lizards: adaptation, phylogenetic inertia, and Nnche tracking. *The American Naturalist*, **174**, 204–220.

Labra, A., Soto-Gamboa, M. & Bozinovic, F. (2001) Behavioral and physiological thermoregulation of Atacama desert-dwelling *Liolaemus* lizards. *Ecoscience*, **8**.

Lailvaux, S.P., Alexander, G.J. & Whiting, M.J. (2003) Sex-based differences and similarities in locomotor performance, thermal preferences, and escape behaviour in the lizard *Platysaurus intermedius wilhelmi*. *Physiological and Biochemical Zoology*, **76**, 511–521.

Lemos-Espinal, J.A. & Ballinger, R.E. (1995) Comparative thermal ecology of the high altitude lizard, *Sceloporus grammicus*. *Canadian Journal of Zoology-Revue Canadienne De Zoologie*, **73**, 2184–2191.

Lemos-Espinal, J.A., Smith, G.R. & Ballinger, R.E. (2002) Body temperature and sexual dimorphism of *Sceloporus aeneus* and *Sceloporus palaciosi* from México. *Amphibia-Reptilia*, **23**, 114–119.

Lemos-Espinal, J.A., Smith, G.R. & Ballinger, R.E. (2003) Ecology of *Xenosaurus grandis agrenon*, a knob-scaled lizard from Oaxaca, Mexico. *Journal of Herpetology*, **37**, 192–196.

Lemos-Espinal, J.A., Smith, G.R. & Ballinger, R.E. (2001) Sexual dimorphism and body temperatures of *Sceloporus siniferus* from Guerrero Mexico. *Western North American Naturalist*, **61**, 498–500.

Lemos-Espinal, J.A., Smith, G.R. & Ballinger, R.E. (1997) Thermal ecology of the lizard, *Sceloporus gadoviae*, in an arid tropical scrub forest. *Journal of Arid Environments*, **35**, 311–319.

Lemos-Espinal, J.A., Ballinger, R.E. & Javelly-Gurría, J.M. (1993) Observations on the sensitivity to high temperatures in two lizard species (*Ameiva undulata* and *Sceloporus horridus*) from Zacatepec, Morelos, Mexico. *Bulletin of the Maryland Herpetological Society*, **29**, 24–29.

Lemos-Espinal, J.A., Smith, G.R. & Ballinger, R.E. (2997) Body temperatures of the Mexican lizard *Sceloporus ochoteranae* from two populations in Guerrero, Mexico. *Herpetological Journal*, **7**, 74–76.

Lemos-Espinal, J.A., Smith, G.R. & Ballinger, R.E. (1997) Observations on the body temperatures and natural history of some Mexican reptiles. *Bulletin of the Maryland Herpetological Society*, **33**, 159–164.

Manzur, M.I. & Fuentes, E.R. (1979) Polygyny and agonistic behavior in the tree-dwelling lizard *Liolaemus tenuis* (Iguanidae). *Behavioral Ecology and Sociobiology*, **6**, 23–28.

Martin, J. & Lopez, P. (2010) Thermal constraints of refuge use by Schreiber’s green lizards, *Lacerta* *schreiberi*. *Behaviour*, **147**, 275–284.

Martín, J. & Salvador, A. (1993) Thermoregulatory behaviour of rock lizards in response to tail loss. *Behaviour*, **124**, 123–136.

Martori, R., Aun, L. & Orlandini, S. (2002) Relaciones térmicas en una población de *Liolaemus koslowskyi*. *Cuadernos de Herpetología*, **16**.

McConnachie, S., Alexander, G.J. & Whiting, M.J. (2009) Selected body temperature and thermoregulatory behavior in the sit-and-wait foraging lizard *Pseudocordylus melanotus melanotus*. *Herpetological Monographs*, **23**, 108–122.

Medina, M., Gutierrez, J., Scolaro, A. & Ibarguengoytia, N.R. (2009a) Thermal responses to environmental constraints in two populations of the oviparous lizard *Liolaemus bibronii* in Patagonia, Argentina. *Journal of Thermal Biology*, **34**, 32–40.

Medina, M., Scolaro, A., Méndez-De la Cruz, F., Sinervo, B. & Ibargüengoytía, N. (2011) Thermal relationships between body temperature and environment conditions set upper distributional limits on oviparous species. *Journal of Thermal Biology*, **36**, 527–534.

Medina, M., Scolaro, A., Mendez-De la Cruz, F., Sinervo, B., Miles, D.B. & Ibarguengoytia, N. (2009b) Thermal biology of genus *Liolaemus*: a phylogenetic approach reveals advantages of the genus to survive climate change. *Journal of Thermal Biology*, **37**, 579–586.

Melville, J. & Schulte, J.A. (2001) Correlates of active body temperatures and microhabitat occupation in nine species of central Australian agamid lizards. *Austral Ecology*, **26**, 660–669.

Menezes, V.A. & Rocha, C.F.D. (2010) Thermal ecology of five *Cnemidophorus* species (Squamata: Teiidae) in east coast of Brazil. *Journal of Thermal Biology*, **36**, 232–238.

Mesquita, D.O. & Colli, G.R. (2003) Geographical variation in the ecology of populations of some Brazilian species of *Cnemidophorus* (Squamata, Teiidae). *Copeia*, **2003**, 285–298.

Mesquita, D.O., Colli, G.R., Costa, G.C., Franca, F.G.R., Garda, A.A. & Peres, A.K. (2006a) At the water's edge: ecology of semiaquatic teiids in Brazilian Amazon. *Journal of Herpetology*, **40**, 221–229.

Mesquita, D.O., Colli, G.R., Franca, F.G.R. & Vitt, L.J. (2006b) Ecology of a cerrado lizard assemblage in the Jalapao region of Brazil. *Copeia*, **2006**, 460–471.

Mesquita, D.O., Costa, G.C. & Colli, G.R. (2006c) Ecology of an amazonian savanna lizard assemblage in Monte Algre, Pará State, Brazil. *South American Journal of Herpetology*, **1**, 61–71.

Miranda, J.P., Ricci-Lobao, A. & Rocha, C.F.D. (2010) Influence of structural habitat use on the thermal ecology of *Gonatodes humeralis* (Squamata: Gekkonidae) from a transitional forest in Maranhao, Brazil. *Zoologia*, **27**, 35–39.

Monasterio, C., Salvador, A., Iraeta, P. & Dıaz, J.A. (2009) The effects of thermal biology and refuge availability on the restricted distribution of an alpine lizard. *Journal of Biogeography*, **36**, 1673–1684.

Navarro-Garcia, J.C., Garcia, A. & Mendez de la Cruz, F.R. (2008) Seasonality, thermoregulation effectiveness of *Aspidoscelis lineatissima* (Sauria: Teiidae) and the thermal quality of a seasonally dry tropical forest in Chamela, Jalisco, Mexico. *Revista Mexicana de Biodiversidad*, **79**.

Perez-Mellado, V. & de la Riva, I. (1998) Sexual size dimorphism and ecology: the case of a tropical lizard, *Tropidurus melanopleurus* (Sauria: Tropiduridae). *Copeia*, **1993**, 969–976.

Philipp, K.M., Böhme, W. & Ziegler, T. (1999) The identity of *Varanus indicus*: redefinition and description of a sibling species coexisting at the type locality (Sauria: Varanidae: *Varanus indicus* group). *Spixiana*, **22**, 273–287.

Pianka, E.R. (2994) Comparative ecology of *Varanus* in the Great Victoria desert. *Australian Journal of Ecology*, **19**, 395–408.

Punzo, F. (2001) Studies on the natural history and ecology of sympatric whiptail lizards (*Cnemidophorus marmoratus* and *C. tesselatus*) from Madera Canyon (Brewster County, Texas). *Texas Journal of Science*, **53**, 43–54.

Sales, R.F.D., Ribeiro, L.B., Jorge, J.S. & Freire, E.M.X. (2011) Habitat use, daily activity periods, and thermal ecology of *Ameiva ameiva* (Squamata: Teiidae) in a caatinga area of northeastern Brazil. *Phyllomedusa*, **10**, 165–176.

Sepulveda, M., Visal, M.A., Farina, J.M. & Sabat, P. (2008) Seasonal and geographic variation in thermal biology of the lizard *Microlophus atacamensis* (Squamata: Tropiduridae). *Journal of Thermal Biology*, **33**, 141–148.

Singh, S., Smyth, A.K. & Blomberg, S.P. (2002) Thermal ecology and structural habitat use of two sympatric lizards (*Carlia vivax* and *Lygisaurus foliorum*) in subtropical Australia. *Austral Ecology*, **27**, 616–623.

Smith, G.R. & Lemos-Espinal, J.A. (2005) Comparative escape behavior of four species of Mexican phrynosomatid lizards. *Herpetologica*, **61**, 225–232.

Smith, H.M. (1939) The Mexican and Central American lizards of the genus *Sceloporus*. *Field Museum of Natural History*, **26**, 1–397.

Smith, J.G., Christian, K. & Green, B. (2008) Physiological ecology of the mangrove-dwelling varanid *Varanus indicus*. *Physiological and Biochemical Zoology*, **81**, 561–569.

Stellatelli, O.A., Block, C., Moreno-Azócar, D.L., Vega, L.E., Isacch, J.P. & Cruz, F.B. (2016) Scale dependency of *Liolaemus* lizards' home range in response to different environmental variables. *Current Zoology*, **62**, 521–530.

Trujillo-Cornejo, F.J. (2001) El medio ambiente térmico y la efectividad de la termorregulación en relación con la evolución del tipo de paridad de las lagartijas *Sceloporus bicanthalis* y *Sceloporus aeneus*. BSc Dissertation, Universidad Nacional Autónoma de México.

Truter, J.C. (2011) Aspects of the thermal ecology of the group-living lizard, *Cordylus cataphractus*: A spatial and temporal analysis.

Ugueto, G.N., Harvey, M.B. & Rivas, G. a. (2009) Two new species of *Cnemidophorus* (Squamata: Teiidae) from islands of the northeastern coast of Venezuela. *Herpetological Monographs*, **23**, 123–153.

Verwaijen, D. & Van Damme, R. (2007) Correlated evolution of thermal characteristics and foraging strategy in lacertid lizards. *Journal of Thermal Biology*, **32**, 388–395.

Vidal, M., Ortiz, J.C. & Labra, A. (2002) Sexual and age differences in ecological variables of the lizard *Microlophus atacamensis* (Tropiduridae) from northern Chile. *Revista Chilena de Historia Natural*, **75**, 283–292.

Villavicencio, H.J., Acosta, J.C., Marinero, J.A. & Canovas, M.G. (2007) Thermal ecology of a population of the lizard, *Liolaemus pseudoanomalus* in western Argentina. *Amphibia-Reptilia*, **28**, 163–165.

Vitt, L.J. & Avila-Pires, T.C.S. (1998) Ecology of two sympatric species of *Neusticurus* (Sauria: Gymnophthalmidae) in the western Amazon of Brazil. *Copeia*, **1998**, 570–582.

Vitt, L.J., Avila-Pires, T.C.S., Esposito, M.C., Sartorius, S.S. & Zani, P.A. (2003) Sharing Amazonian rain-forest trees: ecology of *Anolis punctatus* and *Anolis transversalis* (Squamata: Polychrotidae). *Journal of Herpetology*, **37**, 276–285.

Vitt, L.J. & de Carvalho, C.M. (1992) Life in the trees: the ecology and life history of *Kentropyx striatus* (Teiidae) in the lavrado area of Roraima, Brazil, with comments on the life histories of tropical teiid lizards. *Canadian Journal of Zoology-Revue Canadienne De Zoologie*, **70**, 1995–2006.

Vitt, L.J. & de Carvalho, C.M. (1995) Niche partitioning in a tropical wet season: lizards in the lavrado area of northern Brazil. *Copeia*, **1995**, 305–329.

Vitt, L.J. & Colli, G.R. (1994) Geographical ecology of a neotropical lizard: *Ameiva ameiva* (Teiidae) in Brazil. *Canadian Journal of Zoology-Revue Canadienne De Zoologie*, **72**, 1986–2008.

Vitt, L.J., Shepard, D.B., Vieira, G.H.C., Caldwell, J.P., Colli, G.R. & Mesquita, D.O. (2008) Ecology of Anolis nitens brasiliensis in Cerrado Woodlands of Cantao. *Copeia*, **2008**, 144–153.

Vitt, L.J. & Zani, P.A. (2005) Ecology and reproduction of *Anolis capito* in rain forest of southeastern Nicaragua. *Journal of Herpetology*, **39**, 36–42.

Vitt, L.J. & Zani, P.A. (1996) Ecology of the South American lizard *Norops chrysolepis* (Polychrotidae). *Copeia*, **1996**, 56–68.

Vitt, L.J., Zani, P.A. & Caldwell, J.P. (1996) Behavioural ecology of *Tropidurus hispidus* on isolated rock outcrops in Amazonia. *Journal of Tropical Ecology*, **12**, 81–101.

Woolrich-Pina, G.A., Lemos-Espinal, J.A., Smith, G.R., Oliver-Lopez, L., Correa-Sanchez, F., Altamirano-Alvarez, A., T. & Montoya-Ayala, R. (2012) Thermal ecology of the lizard *Sceloporus gadoviae* (Squamata: Phrynosomatidae) in a semiarid region of southern Puebla, Mexico. *Phyllomedusa*, **11**, 21–27.

Woolrich-Pina, G.A., Smith, G.R. & Lemos-Espinal, J.A. (2011) Body temperatures of two species of

Aspidoscelis from Zapotitlan Salinas, Puebla, Mexico. *Herpetology Notes*, **4**, 387–390.

Woolrich-Piña, G. a, Lemos-Espinal, J. a, Oliver-López, L., Calderón Méndez, M.E., González-Espinoza, J.E., Correa-Sánchez, F. & Montoya Ayala, R. (2006) Ecología térmica de una población de la lagartija *Sceloporus grammicus* (Iguanidae: Phrynosomatinae) que ocurre en la zona centro-oriente de la ciudad de México. *Acta Zoológica Mexicana*, **22**, 137–150.

Zhang, Y.-P. & Ji, X. (2004) The thermal dependence of food assimilation and locomotor performance in southern grass lizards, *Takydromus sexlineatus* (Lacertidae). *Journal of Thermal Biology*, **29**, 45–53.

SUPPLEMENTARY INFORMATION

REMOTE SENSING RESTORES PREDICTABILITY OF ECTOTHERM BODY TEMPERATURE IN THE WORLD'S FORESTS

APPENDIX S1: SUPPLEMENTARY METHODS, TABLES AND FIGURES

Supplementary Methods

Modelling operative temperature (T_e) in full sun

We derived the expected relationships between T_b of a non-thermoregulating lizard at equilibrium with its environment and air temperature, solar radiation, wind speed and shade level by modelling T_e for a theoretical lizard on a flat surface and varying each of these variables individually or jointly, assuming T_b = T_b for a non-thermoregulating lizard at equilibrium. Initial parameters for these calculations are given in Table S1.1. Solar radiation was manipulated by varying latitude while controlling for time of day and year.

We modelled T_e on a flat surface following Buckley (2007) and Sears et al. (2011), using the equation:

$$T_e = T_{air} + \frac{R_{solar} + R_{lw} - \varepsilon_s \sigma (T_{air} + 273)^4}{4\sigma (T_{air} + 273)^3 + c_p \left(1.4 + 0.135\sqrt{\frac{v}{d}}\right)} \qquad \text{Eq S1}$$

where T_{air} is air temperature in degrees Celsius, R_{solar} is absorbed incoming solar (short-wave) radiation, R_{lw} is absorbed long-wave radiation, ε_s is animal emissivity which we set at 0.965, following Buckley (2007), σ is the Stefan-Boltzmann constant (5.67×10^{-8} W m-2 K^{-4}; Buckley 2007), c_p is the specific heat of air (29.3 J mol^{-1} K^{-1}) (Buckley, 2007), *d* is the characteristic dimension of the animal, and *v* is wind velocity. We set *d* equal to the snout-vent length of our theoretical lizard, which assumes the animal is parallel to wind direction (Campbell & Norman, 1998).

We calculated the absorbed long-wave radiation following Buckley's (2007) equation A23:

$$R_{lw} = \alpha_L \left(F_a L_a + F_g L_g\right) \qquad \text{Eq S2}$$

α_L is absorptivity in the long-wave (thermal) waveband, set to 0.965, following Buckley (2007). F_a and F_g are view factors for long-wave radiation from the air and ground, respectively, both set to 0.5 (Buckley, 2007; Sears *et al.*, 2011). L_a is the long-wave radiation from the air, calculated using Buckley's (2007) Eq A21:

$$L_a = \varepsilon_{ac}\sigma(T_{air} + 273)^4 \quad \text{Eq S3}$$

ε_{ac} is clear-sky emissivity which was calculated using Buckley's (2007) equation A12:

$$\varepsilon_{ac} = 9.2 \times 10^{-6}(T_{air} + 273)^2 \quad \text{Eq S4}$$

L_g in Eq S2 is the long-wave radiation from the ground and was calculated following Buckley's (2007) equation A22:

$$L_g = \varepsilon_s\sigma(T_s + 273)^4 \quad \text{Eq S3}$$

where T_s is the ground surface temperature in degrees Celsius and ε_s is the emissivity of the ground. According to Campbell and Norman (1998), emissivity is between 0.95 and 1.0 for most natural surfaces, so we use 0.965, which matches the emissivity of our theoretical lizard.

Solar (short-wave) radiation absorbed by an animal in full sun was modelled following Buckley's (2007) equation A23 (with slightly different notation):

$$R_{solar} = \alpha_s\left(F_pS_p + F_dS_d + F_rS_r\right) \quad \text{Eq S4}$$

In Eq S4, α_s is the absorptivity of solar radiation, set to 0.9 for lizards (Gates, 1980; Buckley, 2007). F_p, F_d, and F_g are view factors between the lizard and direct solar radiation (S_p), diffuse solar radiation (S_d), and reflected solar radiation (S_r), respectively. F_r was set to 0.5 (Buckley, 2007; Sears *et al.*, 2011), as was F_d (Sears *et al.*, 2011). Buckley (2007) set F_d to 0.8, but this slight difference would not affect our conclusions about the shape and direction of the relationships between T_e and microclimate. F_p was modelled following Sears et al.'s (2011) Equation 5 and assumes the lizard is a cylinder with rounded ends:

$$F_p = 1 + \frac{\frac{4h\sin\Theta}{\pi w}}{4 + \frac{4h}{w}} \quad \text{Eq S5}$$

where *h* is the SVL of the lizard (length of cylinder) and *w* is the body width (diameter of cylinder). Θ is the angle between the solar beam and the animal's longitudinal axis, which we assumed to be 90º.

Direct solar radiation reaching the Earth's surface (S_p) in full sun was calculated following Sears et al.'s (2011) equations 6 and 9:

$$S_p = \bar{S}_0 \left(1 + 2 \times \cos\left(\frac{2\pi}{365} J\right)\right) \tau^m \cos z \qquad \text{Eq S6}$$

where $\bar{S}_0$ is the solar constant (1360 W m^{-2}), J Julian day, z is the zenith angle, τ is the optical transmittance of the atmosphere. τ values between 0.6 and 0.7 are typical of clear days (Gates, 1980; Campbell & Norman, 1998), so we set τ=0.65. *m* is the optical air mass number, given by Sears et al. (2011), following Campbell & Norman (1998), as:

$$m = \frac{101.3 e^{\frac{a}{8200}}}{101.3 \cos z} = \frac{e^{\frac{a}{8200}}}{\cos z} \qquad \text{Eq S7}$$

where *a* is elevation in meters above sea level. We calculated zenith angle, assuming a flat surface with no surrounding topography, as a function of latitude, longitude and hour following Sears et al. (2011) and Campbell & Norman (1998):

$$z = \cos^{-1}(\sin \Phi \sin \delta + \cos \Phi \cos \delta \cos h) \qquad \text{Eq S8}$$

where Φ is latitude, δ is solar declination, and *h* is the hour angle of the sun. We calculated declination using Campbell & Norman's(1998) equation 11.2:

$$\delta = 0.39785 \sin(278.97 + 0.9856J + 1.9165 \sin(356.6 + 0.9856J)) \qquad \text{Eq S9}$$

We calculate hour angle of the sun as:

$$h = 15(t - 12 + L_{cor} + E_T) \qquad \text{Eq S10}$$

where *t* is time of day, L_{cor} is a longitudinal correction and E_T is the time equation, calculated from Sears et al. (2011) and Campbell & Norman (1998) as:

$$E_T = 3600^{-1}(-104.7 \sin f + 596.2 \sin 2f + 4.3 \sin 3f - 12.7 \sin 4f$$
$$-429.3 \cos f - 2.0 \cos 2f + 19.3 \cos 3f) \qquad \text{Eq S11}$$

where $f = 279.575 + 0.9856J$. The longitudinal correction (L_{cor}) is the longitude plus 4 minutes for each degree east of a standard meridian (minus 4 minutes for each degree west), where standard meridians are located at 0º, 15º, 30º, . . . , 345º (Campbell & Norman, 1998).

Diffuse solar radiation (S_d) was modelled following Buckley (2007) and Campbell and Norman (1998):

$$S_d = 0.3\bar{S}_0(1 - \tau^m)\cos z \qquad \text{Eq S10}$$

Reflected solar radiation (S_r) was modelled as a function of surface (ground) albedo (α) and the direct and diffuse solar radiation (Campbell & Norman, 1998; Buckley, 2007; Sears *et al.*, 2011):

$$S_r = \alpha\left(S_p + S_d\right) \qquad \text{Eq S10}$$

<u>Modelling operative temperature (T_e) under the forest canopy</u>

Shade has previously been incorporated into T_e models by reducing the amount of solar radiation reaching an animal:

$$T_e = T_{air} + \frac{(1 - S)R_{solar} + R_{lw} - \varepsilon_s\sigma(T_{air} + 273)^4}{4\sigma(T_{air} + 273)^3 + c_p\left(1.4 + 0.135\sqrt{\frac{v}{d}}\right)} \qquad \text{Eq S12}$$

where S is the proportion of an animal in the shade (Sears *et al.*, 2011). However, shade imposed by a forest canopy will affect both solar radiation and long-wave radiation (Campbell, 1986; Campbell & Norman, 1998; Webster *et al.*, 2017). The direct solar radiation reaching an animal in full sun (S_p) was modelled using Equation S4. However, under a forest canopy, only a proportion of the potential direct solar radiation will penetrate the canopy. We modelled the direct solar radiation reaching below the canopy ($S_{p,sub}$) following Campbell and Norman (1998):

$$S_{p,sub} = \omega_p S_p \qquad \text{Eq S13}$$

where ω_p is the proportion of direct solar radiation that makes it through the canopy, which is an exponential function of LAI (Campbell & Norman, 1998):

$$\omega_p = \exp\left(-\sqrt{\alpha_c}K_{b,z}LAI\right) \qquad \text{Eq S14}$$

where α_c is the average absorptivity of the canopy, set to 0.8 (Page 248 in Campbell & Norman, 1998), $K_{b,z}$ is the extinction coefficient for direct solar radiation at zenith angle z. $K_{b,z}$ was modelled as a function of z, assuming a spherical leaf angle distribution (Campbell & Norman, 1998):

$$K_{b,z} = \frac{\sqrt{1 + \tan^2 z}}{2.00132} \quad \text{Eq S15}$$

Diffuse solar radiation below the canopy ($S_{d,sub}$) was found by numerically integrating Equation 15.5 in Campbell and Norman (1998):

$$S_{d,sub} = S_d 2 \int_0^{\frac{\pi}{2}} \exp\left(-\sqrt{\alpha_c} K_{b,z} LAI\right) \sin z \cos z \, dz \quad \text{Eq S16}$$

We then modelled the solar radiation reflected from the ground under the canopy ($S_{r,sub}$) as:

$$S_{r,sub} = \alpha\left(S_{p,sub} + S_{d,sub}\right) \quad \text{Eq S17}$$

and total solar radiation reaching the animal under the canopy ($R_{solar,sub}$) as:

$$R_{solar,sub} = \alpha_s\left(F_p S_{p,sub} + F_d S_{d,sub} + F_r S_{r,sub}\right) \quad \text{Eq S18}$$

The forest canopy will also affect the long-wave radiation incident on an animal if the canopy is a different temperature than the air (Webster *et al.*, 2017). We modelled the below-canopy long-wave radiation ($L_{a,sub}$) following Webster et al. (2017), but accounting for canopy emissivity (ε_c):

$$L_{a,sub} = V_s L_a + (1 - V_s)\varepsilon_c \sigma (T_{can} + 273)^4 \quad \text{Eq S19}$$

where T_{can} is canopy temperature in ºC, V_s is a view factor delineating proportion of radiation comes from clear sky and ε_c is set to 0.99 (Page 273 in Campbell & Norman, 1998). We modelled T_{can} using the empirical relationship derived by Webster et al. (2017):

$$T_{can} = 2.36 + 0.88 T_{air} + 0.0073\left(S_{p,sub} + S_{d,sub} + S_{r,sub}\right) \quad \text{Eq S20}$$

V_s varies between 0 and 1, where 0 indicates complete canopy cover and 1 no canopy cover. We modelled V_s as an exponential function of LAI. When LAI is zero, V_s is 1.0 as all long-wave radiation from the air comes from the sky (there is no canopy). As LAI increases leaves block the sky, decreasing V_s. The proportion of direct (beam) solar radiation that penetrates the canopy (ω_p) is given in Eq S14. This reflects value reflects the amount of direct light reaching the ground between and through leaves (as determined by α_c, canopy absorptivity). Thus, we modelled V_s based on Eq S14, assuming black leaves (α_c=1.0):

$$V_s = \exp(-K_{b,z} LAI) \quad \text{Eq S14}$$

We used these equations to model the expected relationships between air temperature, solar radiation, LAI and wind speed. Parameters used in models, but not defined above are given in Table S1.1.

<u>References</u>

Buckley, L.B. (2007) Linking traits to energetics and population dynamics to predict lizard ranges in changing environments. *The American Naturalist*, **171**, E1–E19.

Campbell, G.S. (1986) Extinction coefficients for radiation in plant canopies calculated using an ellipsoidal inclination angle distribution. *Agricultural and Forest Meteorology*, **36**, 317–321.

Campbell, G.S. & Norman, J.M. (1998) *An introduction to environmental biophysics*, 2nd edn. Springer-Verlag, New York.

Gates, D.M. (1980) *Biophysical Ecology*, Springer-Verlag, New York.

Sears, M.W., Raskin, E. & Angilletta, M.J. (2011) The world is not flat: Defining relevant thermal landscapes in the context of climate change. *Integrative and Comparative Biology*, **51**, 666–675.

Tuanmu, M.N. & Jetz, W. (2014) A global 1-km consensus land-cover product for biodiversity and ecosystem modelling. *Global Ecology and Biogeography*, **23**, 1031–1045.

Webster, C., Rutter, N. & Jonas, T. (2017) Improving representation of canopy temperatures for modeling subcanopy incoming longwave radiation to the snow surface. *Journal of Geophysical Research: Atmospheres*, **122**, 9154–9172.

Table S1.1. Parameter values not given in the supplementary text above for modelling operative temperature of a lizard on a flat surface. Air temperature, wind speed, shade level and latitude (as a proxy for solar radiation) were varied between the given ranges to derive predicted relationships with lizard body temperature. Variable ranges were based on ranges in our global data set

Variable	Default	Range
Air Temperature (ºC)	20	7.7–36.4
Substrate Temperature (ºC)	20	–
Wind speed (m s^{-1})	5	0.14–4.51
Latitude (DD)	34.0	25.5–47.5
Longitude (DD)	-111.0	–
Hour (local time)	11:00	–
Julian Day	10	–
LAI	0	0–6.4
Surface albedo	0.2	–
Elevation (m.a.s.l.)	100	–
Snout-Vent Length (cm)	10	–
Body Diameter (cm)	2	–

Table S1.2. Reclassification of land cover categories in Tuanmu & Jetz (2014) into closed, semi-open and open habitat types.

Class	Description	Habitat type
1	Evergreen/Deciduous Needleleaf Trees	Closed
2	Evergreen Broadleaf Trees	Closed
3	Deciduous Broadleaf Trees	Closed
4	Mixed/Other Trees	Semi-Open
5	Shrubs	Semi-Open
6	Herbaceous Vegetation	Open
7	Cultivated and Managed Vegetation	Open
8	Regularly Flooded Vegetation	Open
9	Urban/Built-up	Open
10	Snow/Ice	-
11	Barren	Open
12	Open Water	-

Table S1.3. Regression of T_b on microclimate and canopy structure for global data and all habitats. For each variable the sign of the coefficient and P-value are given. $P<0.05$ are in bold. All regressions accounted for spatial and phylogenetic autocorrelation. R^2_m (marginal R^2) is the variance explained by predictors and R^2_c (conditional R^2) is the variance explained by predictors, space and phylogeny. T_b is body temperature, Tair is air temperature, SOL is solar radiation, WS is the fifth root of wind speed and LAI is the square root of leaf area index.

Model	Tair	SOL	WS	WS^2	LAI	LAI^2	LAI×SOL	LAI×WS	R^2_m	R^2_c
No LAI										
T_b~Tair +SOL+WS+WS^2	**+; 3e-6**	**+; 0.01**	–; 0.54	+; 0.61					0.13	0.42
T_b~Tair +SOL+WS	**+; 2e-6**	**+;0.01**	–; 0.27						0.13	0.42
T_b~Tair +SOL	**+; 7e-10**	**+; 0.02**							0.13	0.38
With LAI										
T_b~Tair+SOL+WS+WS^2+LAI+LAI^2+ LAI×SOL+LAI×WS	**+; 6e-6**	+; 0.34	–; 0.36	+; 0.44	–; 0.27	+; 0.42	+; 0.49	+; 0.50	0.14	0.43
T_b~Tair+SOL+WS+WS^2+LAI+LAI^2+LAI×SOL	**+; 5e-6**	+; 0.35	–; 0.46	+; 0.52	–; 0.37	+; 0.44	+; 0.50		0.14	0.42
T_b~Tair+SOL+WS+WS^2+LAI+LAI^2	**+; 2e-6**	**+; 0.02**	–; 0.51	+; 0.57	–; 0.46	+; 0.54			0.14	0.40
T_b~Tair+SOL+WS+WS^2+LAI	**+; 3e-6**	**+; 0.02**	–; 0.50	+; 0.57	–; 0.64				0.13	0.42
T_b~Tair+SOL+WS+LAI	**+; 2e-6**	**+; 0.03**	–; 0.27		–; 0.69				0.13	0.41

Table S1.4. Results of final regressions of T_b on microclimate and canopy structure using a Pagel's lambda transformed phylogenetic variance-covariance matrix. For each variable the sign of the coefficient and P-value are given. P<0.05 are in bold. All regressions accounted for spatial and phylogenetic autocorrelation. R^2_m (marginal R^2) is the variance explained by predictors and R^2_c (conditional R^2) is the variance explained by predictors, space and phylogeny. T_b is body temperature, Tair is air temperature, SOL is solar radiation, WS is the fifth root of wind speed and LAI is the square root leaf area index.

	Model	Tair	SOL	WS	LAI	R^2_m	R^2_c
All	T_b~Tair +SOL	**+; 6e-10**	**+; 0.02**			0.13	0.40
Closed	T_b~ LAI				**–; 0.03**	0.15	0.17
Semi	T_b~ Tair	**+; 3e-4**				0.10	0.15
Open	T_b~Tair +SOL	**+; 1e-15**	**+; 4e-3**			0.35	0.52

Table S1.5. Regression of T_b on microclimate and canopy structure for open habitats in the global data. For each variable the sign of the coefficient and P-value are given. P<0.05 are in bold. All regressions accounted for spatial and phylogenetic autocorrelation. R^2_m (marginal R^2) is the variance explained by predictors and R^2_c (conditional R^2) is the variance explained by predictors, space and phylogeny. T_b is body temperature, Tair is air temperature, SOL is solar radiation, WS is the fifth root of wind speed and LAI is the square root leaf area index.

Model	Tair	SOL	WS	WS^2	LAI	LAI^2	LAI×SOL	LAI×WS	R^2_m	R^2_c
					No LAI					
T_b~Tair +SOL+WS+WS^2	**+; 2e-7**	**+; 5e-4**	**–; 0.08**	+; 0.10					0.37	0.64
T_b~Tair +SOL+WS	**+; 2e-9**	**+; 0.001**	–; 0.11						0.36	0.58
T_b~Tair +SOL	**+; 1e-15**	**+; 0.004**							0.35	0.53
					With LAI					
T_b~Tair+SOL+WS+WS^2+LAI+LAI^2+ LAI×SOL+LAI×WS	**+; 1e-6**	+; 0.38	–; 0.16	+; 0.17	–; 0.64	+; 0.09	+; 0.12	–; 0.27	0.40	0.64
T_b~Tair+SOL+WS+WS^2+LAI+LAI^2+LAI×SOL	**+; 7e-7**	+; 0.26	–; 0.07	**+; 0.05**	–; 0.07	+; 0.08	+; 0.19		0.40	0.66
T_b~Tair+SOL+WS+WS^2+ LAI+LAI^2	**+; 5e-8**	**+; 0.002**	–; 0.08	+; 0.10	–; 0.08	+; 0.17			0.39	0.64
T_b~Tair+SOL+WS+WS^2+ LAI	**+; 4e-9**	**+; 0.002**	–; 0.08	+; 0.11	–; 0.21				0.38	0.65

Table S1.6. Regression of T_b on microclimate and canopy structure for semi-open habitats in the global data. For each variable the sign of the coefficient and P-value are given. P<0.05 are in bold. All regressions accounted for spatial and phylogenetic autocorrelation. R^2_m (marginal R^2) is the variance explained by predictors and R^2_c (conditional R^2) is the variance explained by predictors, space and phylogeny. T_b is body temperature, Tair is air temperature, SOL is solar radiation, WS is the fifth root of wind speed and LAI is the square root leaf area index.

Model	Tair	SOL	WS	WS^2	LAI	LAI^2	LAI×SOL	LAI×WS	R^2_m	R^2_c
No LAI										
T_b~Tair +SOL+WS+WS^2	**+; 0.01**	+; 0.70	–; 0.36	+; 0.38					0.11	0.13
T_b~Tair +SOL+WS	**+; 0.004**	+; 0.85	–; 0.71						0.10	0.14
T_b~ Tair+WS	**+; 0.004**		–; 0.73						0.10	0.14
T_b~ Tair	**+; 3e-4**								0.10	0.15
With LAI										
T_b~Tair+SOL+WS+WS^2+LAI+LAI^2+ LAI×SOL+LAI×WS	**+; 0.01**	+; 0.72	–; 0.39	+; 0.37	+; 0.89	+; 0.59	–; 0.75	–; 0.80	0.11	0.19
T_b~Tair+SOL+WS+WS^2+LAI+LAI^2+LAI×SOL	**+; 0.009**	+; 0.71	–; 0.35	+; 0.35	–; 1.0	+; 0.60	–; 0.72		0.11	0.19
T_b~Tair+SOL+WS+WS^2+LAI+LAI^2	**+; 0.009**	+; 0.89	–; 0.31	+; 0.32	–; 0.40	+; 0.45			0.11	0.18
T_b~Tair+SOL+WS+WS^2+LAI	**+; 0.01**	+; 0.83	–; 0.33	+; 0.35	–; 0.69				0.11	0.14
T_b~Tair+SOL+WS+LAI	**+; 0.006**	+; 92	–; 0.71		–; 0.86				0.10	0.15
T_b~Tair+WS+LAI	**+; 0.004**		–; 0.72		–; 0.86				0.10	0.15

Table S1.7. Regression of T_b on microclimate and canopy structure for closed habitats in the global data. For each variable the sign of the coefficient and P-value are given. P<0.05 are in bold. All regressions accounted for spatial and phylogenetic autocorrelation. R^2_m (marginal R^2) is the variance explained by predictors and R^2_c (conditional R^2) is the variance explained by predictors, space and phylogeny. T_b is body temperature, Tair is air temperature, SOL is solar radiation, WS is the fifth root of wind speed and LAI is the square root leaf area index.

Model	Tair	SOL	WS	WS^2	LAI	LAI^2	LAI×SOL	LAI×WS	R^2_m	R^2_c
					No LAI					
T_b~Tair +SOL+WS+WS^2	+; 0.60	+; 0.80	+; 0.58	–; 0.65					0.08	0.09
T_b~Tair +SOL+WS	+; 0.54	+; 0.44	+; 0.29						0.07	0.12
T_b~ SOL+WS		+; 0.35	+; 0.35						0.06	0.13
T_b~ WS			+; 0.38						0.03	0.07
					With LAI					
T_b~Tair+SOL+WS+WS^2+LAI+LAI^2+ LAI×SOL+LAI×WS	–; 0.91	+; 0.32	–; 0.47	–; 0.67	–; 0.53	–; 0.88	–; 0.39	+; 0.08	0.28	0.28
T_b~Tair+SOL+WS+WS^2+LAI+LAI^2+LAI×WS	+; 0.75	+; 0.34	–; 0.52	–; 0.72	–0.16	–; 0.71		+; 0.10	0.27	0.27
T_b~Tair+SOL+WS+WS^2+LAI+LAI^2	+; 1.0	+; 0.95	+; 0.42	–; 0.47	–; 0.73	–; 0.89			0.20	0.20
T_b~Tair+SOL+WS+WS^2+LAI	–; 0.98	+; 0.92	+; 0.40	–; 0.45	**–; 0.04**				0.20	0.20
T_b~Tair+SOL+WS+LAI	+; 0.90	+; 0.40	+; 0.32		**–; 0.05**				0.19	0.19
T_b~SOL+WS+LAI		+; 0.37	+; 0.31		**–; 0.03**				0.20	0.20
T_b~WS+LAI			+; 0.35		**–; 0.03**				0.18	0.18
T_b~LAI					**–; 0.03**				0.15	0.17

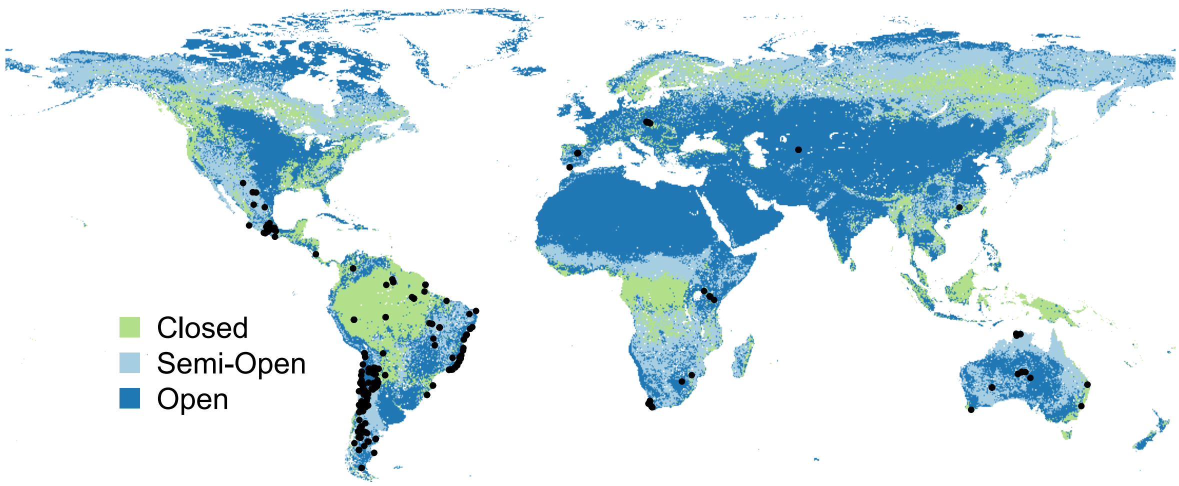

Figure S1.1. Location of lizard populations (n=269) with T_b data, overlaid over our habitat classification.